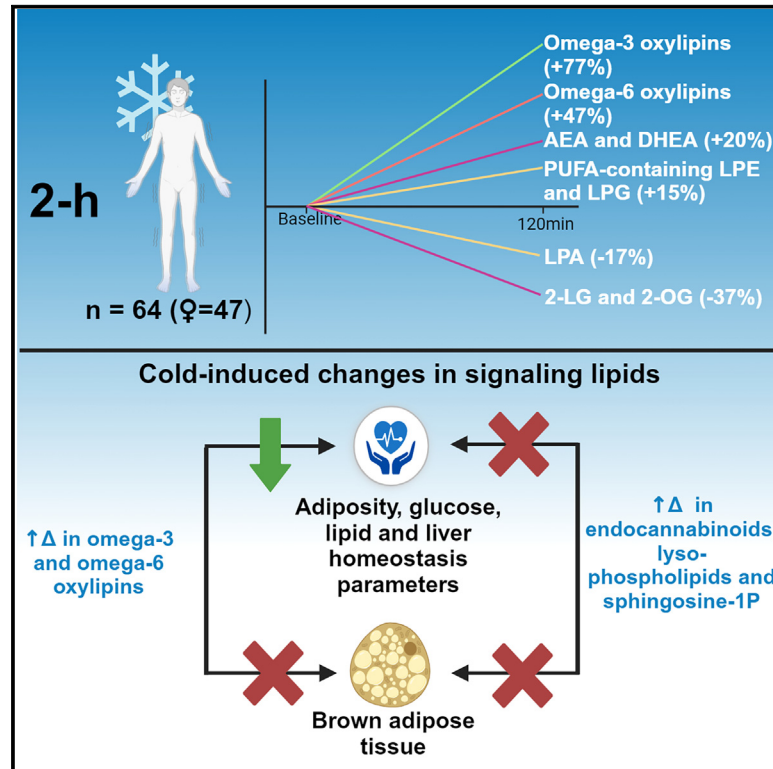


# Cold-induced changes in plasma signaling lipids are associated with a healthier cardiometabolic profile independently of brown adipose tissue

## Graphical abstract



## Authors

Lucas Jurado-Fasoli, Guillermo Sanchez-Delgado, Xinyu Di, ..., Thomas Hankemeier, Jonatan R. Ruiz, Borja Martinez-Tellez

## Correspondence

ruizj@ugr.es (J.R.R.), borjammt@gmail.com (B.M.-T.)

## In brief

Jurado-Fasoli et al. reveal dynamic changes in the levels of signaling lipids in response to 2 h of cold. They also elucidate that cold-induced changes in omega-6 and omega-3 oxylipins are related to a healthier cardiometabolic profile independently of brown fat. The observed changes remain unaltered after a 24-week exercise intervention.

## Highlights

- 2 h of cold exposure modifies the levels of signaling lipids in young adults
- Cold-induced changes in signaling lipids are not related to BAT-related outcomes
- Cold-induced changes in oxylipins are related to a healthier cardiometabolic profile
- 24 weeks of exercise training does not modify the signaling lipid response to cold



## Article

# Cold-induced changes in plasma signaling lipids are associated with a healthier cardiometabolic profile independently of brown adipose tissue

Lucas Jurado-Fasoli,<sup>1,2</sup> Guillermo Sanchez-Delgado,<sup>1,3,4,5</sup> Xinyu Di,<sup>6</sup> Wei Yang,<sup>6</sup> Isabelle Kohler,<sup>7,8</sup> Francesc Villarroya,<sup>4,9</sup> Concepcion M. Aguilera,<sup>4,5,10</sup> Thomas Hankemeier,<sup>6</sup> Jonatan R. Ruiz,<sup>1,4,5,12,13,\*</sup> and Borja Martinez-Tellez<sup>1,4,11,12,\*</sup>

<sup>1</sup>Department of Physical Education and Sports, Faculty of Sports Science, Sport and Health University Research Institute (iMUDS), University of Granada, Carretera de Alfacar s/n, 18071 Granada, Spain

<sup>2</sup>Department of Physiology, Faculty of Medicine, University of Granada, Granada, Spain

<sup>3</sup>Department of Medicine, Division of Endocrinology, Centre de Recherche du Centre Hospitalier Universitaire de Sherbrooke, Université de Sherbrooke, Sherbrooke, QC, Canada

<sup>4</sup>CIBER de Fisiopatología de la Obesidad y Nutrición (CIBEROBN), Instituto de Salud Carlos III, Madrid, Spain

<sup>5</sup>Instituto de Investigación Biosanitaria, Ibs.Granada, Granada, Spain

<sup>6</sup>Metabolomics and Analytics Center, Leiden Academic Centre for Drug Research (LACDR), Leiden University, Leiden, the Netherlands

<sup>7</sup>Vrije Universiteit Amsterdam, Amsterdam Institute of Molecular and Life Sciences (AIMMS), Division of BioAnalytical Chemistry, Amsterdam, the Netherlands

<sup>8</sup>Center for Analytical Sciences Amsterdam, Amsterdam, the Netherlands

<sup>9</sup>Department of Biochemistry and Molecular Biomedicine, Institute of Biomedicine of the University of Barcelona, Barcelona, Spain

<sup>10</sup>Department of Biochemistry and Molecular Biology II, "José Mataix Verdú" Institute of Nutrition and Food Technology (INYTA), Biomedical Research Centre (CIBM), University of Granada, 18016 Granada, Spain

<sup>11</sup>Department of Education, Faculty of Education Sciences and SPORT Research Group (CTS-1024), CERNEP Research Center, University of Almería, Almería, Spain

<sup>12</sup>These authors contributed equally

<sup>13</sup>Lead contact

\*Correspondence: [ruizj@ugr.es](mailto:ruizj@ugr.es) (J.R.R.), [borjammt@gmail.com](mailto:borjammt@gmail.com) (B.M.-T.)

<https://doi.org/10.1016/j.xcrm.2023.101387>

## SUMMARY

Cold exposure activates brown adipose tissue (BAT) and potentially improves cardiometabolic health through the secretion of signaling lipids by BAT. Here, we show that 2 h of cold exposure in young adults increases the levels of omega-6 and omega-3 oxylipins, the endocannabinoids (eCBs) anandamide and docosahexaenoyl ethanolamine, and lysophospholipids containing polyunsaturated fatty acids. Contrarily, it decreases the levels of the eCBs 1-LG and 2-LG and 1-OG and 2-OG, lysophosphatidic acids, and lysophosphatidylethanolamines. Participants overweight or obese show smaller increases in omega-6 and omega-3 oxylipins levels compared to normal weight. We observe that only a small proportion (~4% on average) of the cold-induced changes in the plasma signaling lipids are slightly correlated with BAT volume. However, cold-induced changes in omega-6 and omega-3 oxylipins are negatively correlated with adiposity, glucose homeostasis, lipid profile, and liver parameters. Lastly, a 24-week exercise-based randomized controlled trial does not modify plasma signaling lipid response to cold exposure.

## INTRODUCTION

Cardiometabolic diseases are the leading cause of premature death in the Western world, responsible for over 40% of fatalities.<sup>1–4</sup> These diseases might result from an unhealthy lifestyle that can lead to obesity, which has become so prevalent that it is now at a pandemic level.<sup>1,4</sup> Efficient solutions to reduce the incidence of cardiometabolic diseases and the discovery of new approaches for their treatment are therefore urgently needed.<sup>5,6</sup>

Cold exposure has recently been proposed as an up-and-coming tool in the battle against cardiometabolic diseases<sup>7–9</sup>

since it activates brown adipose tissue (BAT),<sup>10</sup> a thermogenic tissue characterized by its ability to dissipate energy as heat.<sup>5,11,12</sup> Indeed, a human study including >134,000 individuals demonstrated that individuals with detectable BAT (determined through <sup>18</sup>F-fluorodeoxyglucose positron emission tomography/computed tomography scans [<sup>18</sup>F-FDG-PET/CT]) have a 4.9% and 3.1% lower incidence of type 2 diabetes and coronary artery disease, respectively.<sup>13</sup> These findings suggest a favorable impact of human BAT on cardiometabolic health, but it remains unknown how this tissue can exert its beneficial effects.<sup>13</sup> Human brown adipocytes produce so-called batokines, i.e., signaling molecules that may regulate the metabolism and,



thereby, contribute to an improved cardiometabolic profile.<sup>14–16</sup> Hence, the beneficial impact of human BAT on improving cardiometabolic health may be due to its secretory function.<sup>14–16</sup>

Among all potential signaling molecules, a group of signaling lipids known as oxylipins encompasses a few metabolites that have been identified as BAT lipokines. Specifically, the oxylipin 12,13-dihydroxy-9Z-octadecenoic acid (12,13-DiHOME) is considered a BAT lipokine, which can increase the uptake of fatty acids by BAT and skeletal muscle.<sup>17,18</sup> Additionally, the plasma levels of 12,13-DiHOME increased after 2 h of cold exposure<sup>18</sup> and a bout of exercise<sup>17</sup> in humans and mice, suggesting a systemic signaling effect. Likewise, BAT also secretes the oxylipin 12-hydroxyeicosapentaenoic acid (12-HEPE), which enhances glucose uptake in adipose tissue and skeletal muscle, improving glucose tolerance in obese mice.<sup>19</sup> BAT also releases maresin 2 (MaR2), which targets liver macrophages and effectively reduces inflammation in obese mice.<sup>20</sup> Next to oxylipins, endocannabinoids (eCBs) have been also postulated as lipids potentially secreted by BAT *in vitro*.<sup>21</sup> Indeed, short- and long-term cold exposures elevate circulating eCBs and activate genes responsible for eCB metabolism in murine BAT, supporting their role as potential brown fat lipokines.<sup>22</sup> Similarly, after 24 h of cold exposure, BAT lysophospholipid and sphingolipid levels dramatically decreased, whereas these lipids increased in circulation.<sup>23</sup> Further investigations are necessary to fully understand the secretory role of human BAT, given that most signaling lipids recognized as brown fat lipokines have been discovered in mice but not confirmed in humans yet.<sup>17–20,22,23</sup>

Besides cold exposure, exercise is another non-pharmacological approach that may enhance cardiometabolic health and possibly stimulate the activation of BAT in humans.<sup>24</sup> We recently conducted one of the largest exercise-based randomized clinical trials on human BAT physiology<sup>25</sup> and observed no evidence of BAT activation after 24 weeks of a supervised exercise program in young adults. However, we observed a reduction in fat mass and fasting levels of oxylipins and eCBs after the exercise intervention.<sup>25,26</sup> These findings suggest that altering adiposity and circulating levels of signaling lipids through interventions, such as exercise, could potentially regulate the impact of cold exposure on the release of brown fat lipokines. Further exploring how external interventions can potentially modify the secretome function of BAT is therefore clinically relevant.

This study aimed to investigate the impact of a 2-h cold exposure on the plasma signaling lipids of young adults, specifically oxylipins, eCBs and analogs, lysophospholipids, and sphingosine-1-phosphate species. Furthermore, this study investigated the relationship of cold-induced changes in plasma signaling lipids with BAT parameters (i.e., volume, activity, and radiodensity) and cardiometabolic risk factors. Lastly, we examined the impact of a 24-week supervised exercise program on the response of plasma signaling lipids to cold exposure and its correlation with changes in BAT.

## RESULTS

Among the initial 145 selected participants, we collected blood samples and measured plasma signaling lipids in 64 individuals

before and during 2 h of cold exposure (Figure 1). From these 64 participants (see phenotypical traits in Table 1), 30 completed the exercise intervention and had their blood samples collected in response to cold exposure after the intervention. These subjects were thus included in subsequent analyses (Figure S2, see phenotypical traits in Table S5).

### 2-h cold exposure modifies the levels of signaling lipids

A 2-h cold exposure increased the levels of omega-6 polyunsaturated fatty acids (PUFAs) linoleic acid (LA), dihomo- $\gamma$ -linolenic acid (DGLA), and arachidonic acid (AA), as well as their derived oxylipins (32 out of 39 omega-6 PUFAs; an average increase of +46.9%; all  $p \leq 0.04$ ; Figure 2A). Likewise, omega-3 PUFAs  $\alpha$ -linolenic acid (ALA), eicosapentaenoic acid (EPA), and docosahexaenoic acid (DHA), as well as their derived oxylipins increased after cold exposure (17 out of 17 omega-3 PUFAs; average +77.4%; all  $p < 0.001$ ; Figure 2B). In contrast, cold exposure decreased the levels of the omega-6 oxylipin 9,12,13-TriHOME (–13.2%;  $p = 0.003$ ; Figure 2A). Overall, these analyses revealed that platelet-related omega-6 oxylipins (i.e., 12-HHTrE, thromboxane<sub>B2</sub>, and 12-HETE; Figure 2A; average +185%) and DHA-derived omega-3 oxylipins (Figure 2B; average +89.6%) were the groups of lipids that showed the largest increase. Moreover, cold exposure increased the levels of the two eCBs, anandamide (AEA) and docosahexaenylethanolamide (DHEA) (2 out of 5 eCBs; average +19.5%), whereas it decreased the analogs 1-LG and 2-LG and 1-OG and 2-OG (2 out of 5 eCBs; average –37.4%; all  $p \leq 0.001$ ; Figure 2C). In addition, the levels of lysophosphatidic acid (LPA) decreased after cold exposure (9 out of 11 LPAs average –17.2%; all  $p \leq 0.01$ ; Figure 2D). Contrarily, the levels of PUFA-containing lysophosphatidylethanolamine (LPE) (6 out of 13 LPEs; +15.4%), PUFA-containing lysophosphatidylglycerol (LPG) (3 out of 9 LPGs; +9.4%), and lysophosphatidylserine (LPS) (3/3; +33.5%) increased significantly in response to cold (all  $p \leq 0.04$ ; Figure 2D). These results persisted when we repeated the analyses separately for men (Figure S3) and women (Figure S4), in participants with normal weight (Figure S5), as well as participants overweight or obese (Figure S6). It is worth mentioning that the levels of omega-6 and omega-3 oxylipins increased to a greater extent in response to cold (+58.0% and +81.9%, respectively) in participants with normal weight compared with participants overweight or obese (+31.6% and +69.9%, respectively) (Figures S5, S6, and S7).

### Cold-induced changes in the levels of signaling lipids are not markedly related to brown adipose tissue

Next, we observed that only a small proportion (~4% on average) of the cold-induced changes in the plasma of signaling lipids was slightly correlated with BAT parameters (Figure 3). Cold-induced changes in plasma levels of omega-6 (i.e., LA, GLA, DGLA, AA, and adrenic acid [AdRA]) and omega-3 PUFAs (i.e., ALA, DALA, and EPA) were negatively correlated with BAT volume (8 out of 105 lipids; 7.6%; all  $r \leq -0.32$  and  $p \leq 0.04$ ; Figure 3A). Similarly, we also observed a negative correlation between cold-induced changes in levels of 5-HETrE and 15-HETrE (i.e., DGLA-derived oxylipins) and BAT volume (2 out of 105 lipids; 1.9%; both  $r \leq -0.32$  and  $p \leq 0.03$ ; Figure 3A). We found

**Table 1. Baseline characteristics of the study participants**

	All (n = 64)		Men (n = 17)		Women (n = 47)	
	mean	SD	mean	SD	mean	SD
Age (years)	21.8	2.2	22.4	2.4	21.6	2.1
<i>Body composition</i>						
BMI (kg/m <sup>2</sup> )	24.6	4.8	26.9	6.21	23.76	3.93
Waist circumference (cm)	80.7	14.6	90.9	18.2	76.9	11.0
Lean mass (kg)	41.3	9.2	52.9	7.5	37.0	5.3
Fat mass (kg)	25.1	9.6	26.3	14.3	24.6	7.3
Fat mass (%)	35.9	7.8	30.1	9.8	38.0	5.7
VAT mass (g)	320.7	189.3	441.2	218.1	277.1	158.8
<i>Cardiometabolic risk factors</i>						
Glucose (mg/dL)	88.1	6.8	89.7	9.4	87.5	5.5
Insulin (μIU/mL)	8.5	6.5	10.7	10.6	7.7	4.0
HOMA-IR	1.9	1.8	2.5	3.0	1.7	1.0
Total cholesterol (mg/dL)	165.9	37.4	160.7	47.5	167.9	33.4
HDL-C (mg/dL)	54.1	11.5	46.2	6.5	57.0	11.7
LDL-C (mg/dL)	95.8	29.4	94.9	36.5	96.1	26.8
Triglycerides (mg/dL)	86.9	63.8	102.4	81.4	81.2	56.0
APOA1 (mg/dL)	149.8	33.1	128.7	17.6	155.7	34.2
APOB (mg/dL)	65.7	20.1	65.0	24.8	65.9	19.0
Leptin (μg/L)	6.2	4.4	3.5	3.4	7.1	4.4
Adiponectin (mg/L)	11.4	8.2	8.0	5.7	12.7	8.6
GPT (IU/L)	19.3	19.0	30.7	31.5	15.0	8.3
GGT (IU/L)	19.81	21.57	32.76	34.85	14.91	10.7
ALP (IU/L)	74.75	23.10	86.47	27.28	70.41	19.9
C-reactive protein (mg/L)	2.7	3.9	2.8	3.1	2.6	4.2
<i>Brown adipose tissue</i>						
BAT volume (mL)	67.6	61.6	80.6	76.9	62.8	55.3
BAT SUV <sub>mean</sub>	3.6	1.8	3.3	1.2	3.7	2.0
BAT SUV <sub>peak</sub>	10.7	7.7	10.1	7.7	10.9	7.8
BAT radiodensity (HU)	-59.2	8.4	-58.9	8.5	-59.3	8.5

Data are presented as mean and standard deviation (SD). BAT radiodensity sample size: all, n = 47; men, n = 13; women, n = 34. Abbreviations are as follows: ALP, alkaline phosphatase; APOA1, apolipoprotein A1; APOB, apolipoprotein B; BAT, brown adipose tissue; BMI, body mass index; GGT, gamma-glutamyl transferase; GPP, glutamic pyruvic transaminase; HDL-C, high-density lipoprotein cholesterol; HOMA-IR, homeostatic model assessment of insulin resistance index; HU, Hounsfield Units; LDL-C, low-density lipoprotein cholesterol; SUV, standardized uptake value; VAT, visceral adipose tissue.

a positive correlation between cold-induced changes in levels of LPE (16:0) and platelet-activating factor (PAF) (16:0) and BAT volume (2 out of 105 lipids; 1.9%; both  $r \geq 0.32$  and  $p \leq 0.04$ ; Figure 3A). However, no significant correlations were observed between cold-induced plasma signaling lipid changes and BAT SUV<sub>mean</sub> (all  $p > 0.05$ ; Figure 3B). We found that cold-induced changes in LA levels were negatively correlated with BAT SUV<sub>peak</sub> ( $r = -0.32$  and  $p = 0.02$ ), whereas 1-AG and 2-AG plasma levels were positively correlated ( $r = 0.32$  and  $p = 0.04$ ) (Figure 3C). Lastly, cold-induced changes in LPA (20:3, 22:4), LPE (22:5), and lysophosphatidylinositol (16:0) were positively correlated with BAT mean radiodensity (4 out of 105 lipids; 3.8%; all  $r \geq 0.33$  and  $p \leq 0.03$ ; Figure 3D). These significant results disappeared when correlation analyses were performed in only men (Figure S8) and individuals overweight or obese (Figure S11). In

women (Figure S9) and individuals with normal weight (Figure S10), the significance of most of the correlations also disappeared, except for LA, GLA, and 5-HETrE, which were still negatively correlated with BAT volume.

#### Cold-induced changes in the levels of omega-6 and omega-3 oxylipins are related to a healthier cardiometabolic profile

We found that a large proportion of cold-induced changes in the levels of omega-6 and omega-3 oxylipins was associated with a healthier cardiometabolic profile (Figures 4A and 4B). On average, ~45% of cold-induced changes in omega-6 and omega-3 oxylipins were negatively correlated with markers of adiposity (i.e., body mass index [BMI], waist circumference, FM, and visceral adipose tissue), ~30% with glucose

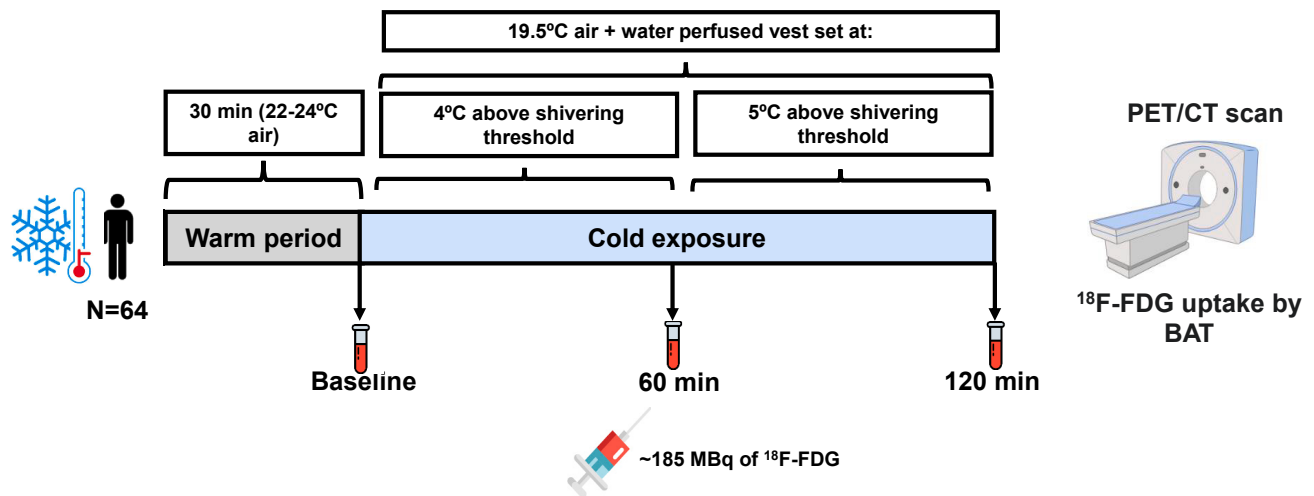


**Figure 1. Design of the study investigating the effects of a 2-h cold exposure on the plasma levels of signaling lipids in young adults**  
Abbreviations are as follows:  $^{18}\text{F}$ -FDG,  $^{18}\text{F}$ -fluorodeoxyglucose; BAT, brown adipose tissue; PET/CT, positron emission tomography/computed tomography.

homeostasis parameters (i.e., glucose, insulin, and homeostatic model assessment of insulin resistance index),  $\sim 60\%$  with lipid profile parameters (i.e., total cholesterol, low-density lipoprotein cholesterol [LDL-C], triglycerides, and apolipoprotein B [APOB]), and  $\sim 35\%$  with liver parameters (i.e., glutamic pyruvic transaminase and gamma-glutamyl transferase) (Figures 4A, 4B, and S12). In contrast, overall cold-induced changes in eCBs and analogs, lysophospholipids, and sphingosine-1-phosphate species were not correlated with cardiometabolic risk factors (Figures 4C and 4D). The correlations between cold-induced changes in omega-6 and omega-3 oxylipins and cardiometabolic risk factors were similar when we repeated the analyses separately in men (Figures S13A and S13B) and women (Figures S14A and S14B). However, when we repeated the analyses separately in participants with normal weight (Figures S15A and S15B) and overweight or obese (Figures S16A and S16B), a large proportion of cold-induced changes in omega-6 and omega-3 oxylipins was correlated with lipid profile parameters (i.e., total cholesterol, LDL-C, triglycerides, and APOB; normal weight  $\sim 33\%$ ; overweight or obesity  $\sim 13\%$ , on average) but surprisingly not with adiposity, glucose homeostasis, and liver parameters.

Additionally, a higher water temperature was related to higher changes in signaling lipids. However, we found that cold-induced changes in only 5 out of 105 lipids (4.7%, Figure S17A) were slightly related to the water temperature of the cooling vest (i.e., cold-induced changes in men 6.6% [Figure S17B], in women 0.9% [Figure S17C], in normal weight 3.8% [Figure S17D], and overweight or obese 5.7% [Figure S18E], respectively). The association between the proportion of cold-induced changes in signaling lipids with cardiometabolic parameters was not affected by the inclusion of water temperature as a confounder (Figure S18). Lastly, the correlations between cold-induced changes in omega-6 and omega-3 oxylipins and cardiometabolic risk factors were similar when we adjusted the analyses for BAT volume or BAT SUVpeak (data not shown).

The aforementioned analyses were repeated using the 60-min fold change compared to the baseline for all signaling lipids, instead of the 120-min fold change relative to the baseline; the results remained unaltered (data not shown).

#### A 24-week supervised concurrent exercise intervention does not modify the plasma signaling lipid response to cold exposure

Lastly, we examined whether a 24-week supervised concurrent exercise program, which reduced the levels of signaling lipids in the blood and improved the cardiometabolic profile of the participants in this study,<sup>25,26</sup> modified the cold-induced changes in the plasma signaling lipids. We found that after 24 weeks of the exercise program, neither moderate-intensity nor vigorous-intensity regime significantly modified the response of bioactive lipids to cold exposure compared to the control group (all  $p > 0.05$ ; Figure 5). Additionally, these cold-induced changes in the plasma signaling lipids were unrelated to BAT changes (i.e., after 24 weeks *minus* baseline; data not shown).

#### DISCUSSION

The current study reveals that 2 h of cold exposure induced changes in the levels of signaling lipids (i.e., omega-6 and omega-3 oxylipins, eCBs and analogs, lysophospholipids, and sphingosine-1-phosphate species) in young adults. Moreover, we found that cold-induced changes in omega-6 and omega-3 oxylipins were related to a healthier cardiometabolic profile (i.e., lower adiposity, glucose, lipid, and liver parameters) independently of BAT, in both men and women. Indeed, participants overweight or obese showed smaller increases in omega-6 and omega-3 oxylipins levels in response to cold (+31.6% and +69.9%, respectively) compared to participants with normal weight (+58.0% and +81.9%, respectively). These results suggest that individuals with higher adiposity and cardiometabolic risk factors have impaired secretion of these lipids in response

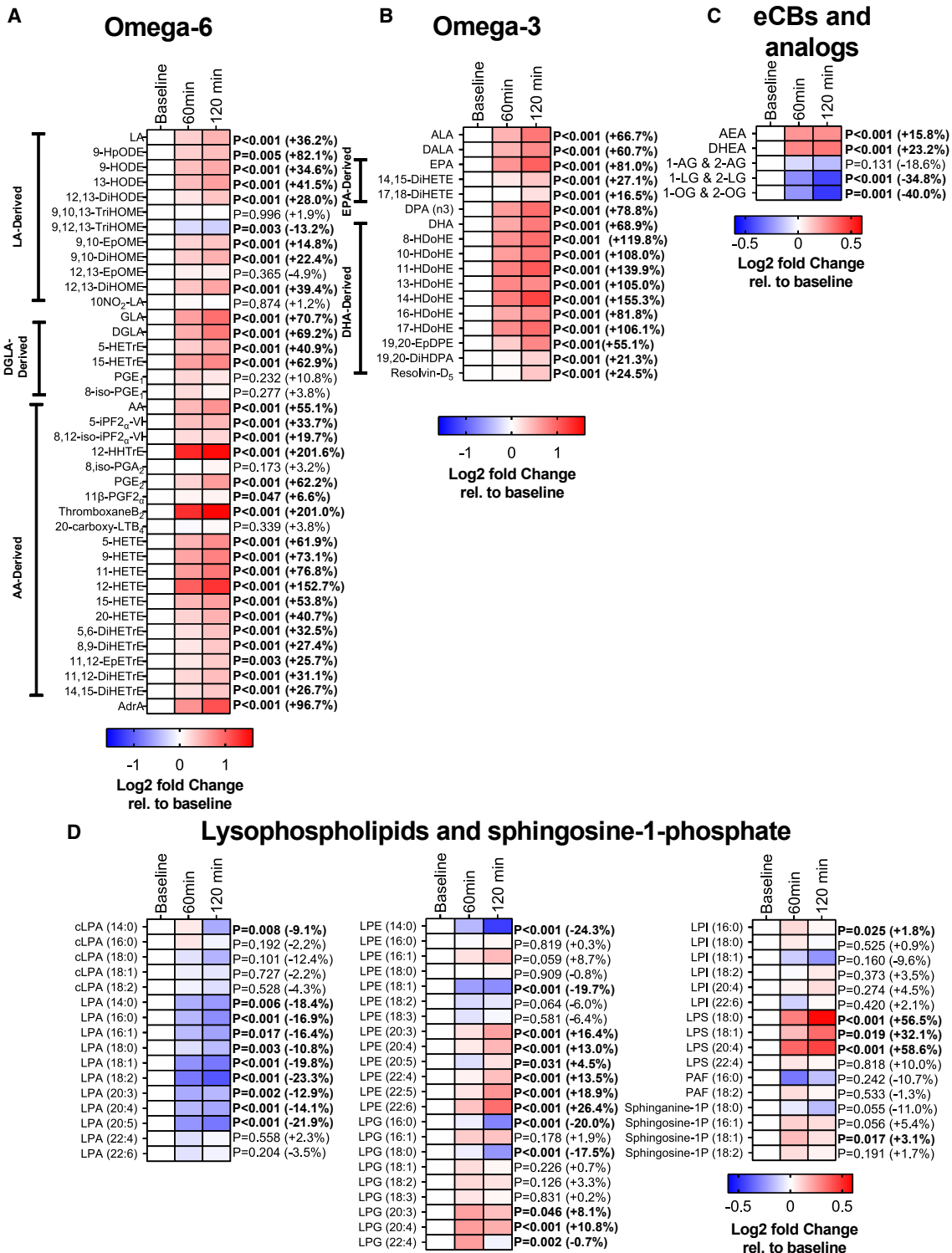


**Figure 2. 2-h cold exposure modifies the levels of signaling lipids**

Effects of 2-h cold exposure on the plasma levels of omega-6 oxylipins (A), omega-3 oxylipins (B), endocannabinoids and analogs (eCBs, C), and lysophospholipids and sphingosine-1-phosphate (D) in young adults. The colors of the squares represent the mean log<sub>2</sub> fold change of the area peak ratio of that time point relative to baseline. Red color represents an increase, whereas blue represents a decrease. p values were obtained from repeated measures analyses of variance (ANOVA). Values in brackets represent the percentage of change at 120 min relative to baseline. The name and abbreviations of signaling lipids are detailed in Table S3.

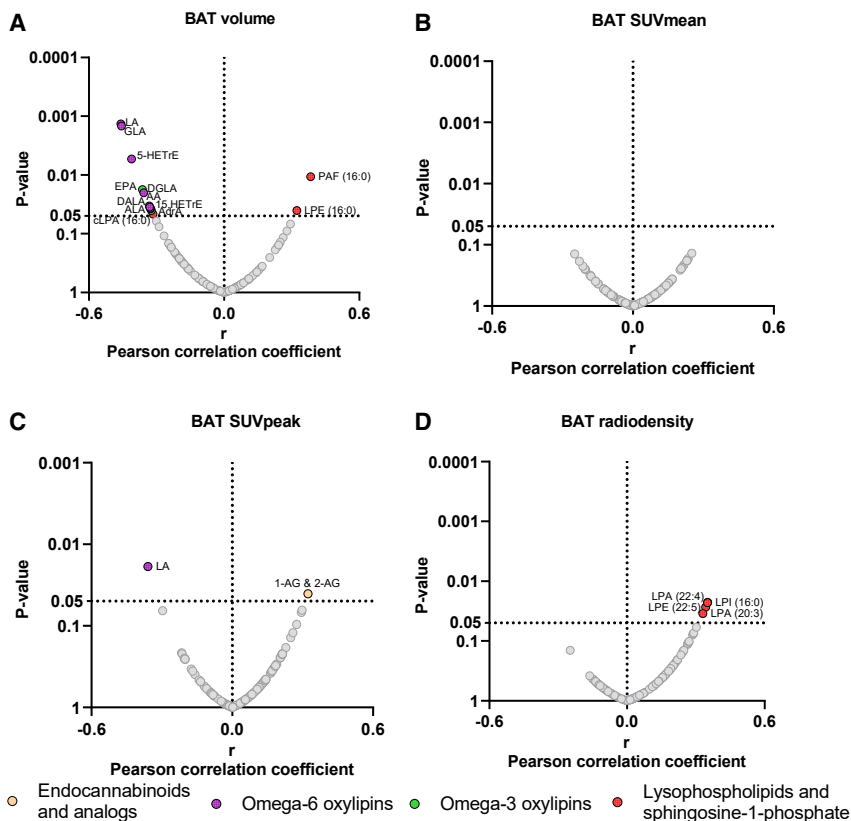


**Figure 3. Association between cold-induced changes in the plasma levels of signaling lipids and brown adipose tissue-related outcomes**

Volcano plots show partial correlation analyses between the 120-min fold change relative to baseline and BAT volume (A), BAT SUVmean (B), BAT SUVpeak (C), and BAT mean radiodensity (D,  $n = 47$ ). Partial correlation analyses were adjusted for the natural calendar day when the baseline PET/CT scan was performed. The X axis represents Pearson partial correlation coefficients, whereas the Y axis represents the false discovery rate (FDR)-adjusted p values of the correlations. Gray dots represent non-significant correlations, whereas colored dots represent statistically significant correlations ( $p$  value  $< 0.05$  after FDR correction). Abbreviations are as follows: BAT, brown adipose tissue; eCBs, endocannabinoids; SUV, standardized uptake value.

to cold exposure. Lastly, although the 24-week exercise intervention decreased adiposity and fasting levels of oxylipins and eCBs,<sup>25,26</sup> it did not modify the plasma signaling lipid response to cold exposure, suggesting that other factors may regulate these responses.

### Role of cold exposure on the levels of signaling lipids

In the present study conducted in young adults, a 2-h cold exposure increased the plasma levels of 80% of the omega-6 (by +46.9%) and 100% of omega-3 (by +77.4%) oxylipins measured. Cold exposure increases sympathetic activation releasing fatty acids (e.g., PUFAs) from white adipose tissue into circulation<sup>27</sup> and increases immune cell counts and inflammatory cytokines (e.g., interleukin-6).<sup>28–30</sup> PUFAs are the precursors of oxylipins, which are produced mainly by non-enzymatic oxidative stress action or by the action of cyclooxygenases, lipoxygenases, and cytochrome P450 enzymes. These enzymes are found in the blood, immune cells, platelets, skeletal and smooth muscle, skin, brain, kidney, and liver among other tissues, but the physiological response in these tissues is unknown since oxylipins were measured in plasma.<sup>31–34</sup> Thus, upon cold exposure, omega-6 oxylipins (i.e., AA-derived eicosanoids) may act as a pro-inflammatory response, whereas omega-3 oxylipins (i.e., EPA- and DHA-derived specialized pro-resolving lipid mediators) may act as an anti-inflammatory and pro-resolution response to restore the inflammatory and immune status.<sup>31,35–37</sup>

Next to oxylipins, PUFAs can also be the precursor of eCBs.<sup>38–40</sup> Cold stimulation increases eCB and analog levels

(i.e., AEA, 2-AG, OEA, and PEA) in mice's BAT and white adipose tissue.<sup>22</sup> However, we found that AEA and DHEA increased (+19.5%), whereas 1-LG and 2-LG and 1-OG and 2-OG decreased (−37.4%). AEA and DHEA are partial agonists of the cannabinoid-1 receptor 39, whose density increased in BAT of lean men after 2 h of cold exposure.<sup>41</sup> Contrarily, 1-LG and 2-LG and 1-OG and 2-OG bind the G protein-coupled receptor 119 39.

AEA increase might be related to glucose and lipid metabolism homeostasis.<sup>39</sup> Similarly to oxylipins, DHEA might have anti-inflammatory effects,<sup>40</sup> and 1-OG and 2-OG might have inflammatory/immune functions (i.e., nuclear factor- $\kappa$ B signaling in macrophages).<sup>42</sup> The different response upon cold exposure in the plasma levels of AEA and DHEA vs. 1-LG and 2-LG and 1-OG and 2-OG is intriguing. In this sense, 1-LG and 2-LG moderately inhibit the activity of 2-AG and AEA.<sup>39</sup> Therefore, it seems plausible that upon cold exposure, there is a synergy effect decreasing 1-LG and 2-LG levels to potentiate the 2-AG effects (which increased upon cold exposure in our study participants). In addition, 1-OG and 2-OG are mainly found in the intestinal lumen and are produced as an intermediate of lipid digestion, concretely the oleic acid.<sup>39</sup> Thus, its decrement could be explained by the fact that participants were in a fasted state, and also that cold exposure is a sympathetic stimulus that decreases splenic blood flow and inhibits gastrointestinal muscle activity and digestion.<sup>43</sup> Alternatively, it may also be possible that 1-LG and 2-LG and 1-OG and 2-OG peaked earlier in the plasma in response to cold exposure, and we have missed this effect since we have only collected plasma before and 1 and 2 h after. However, with our study design, these hypotheses remain speculative, and further mechanistic studies should investigate the differential response upon cold exposure in the levels of eCBs analog species.

A 2-h cold exposure also increased PUFA-containing LPE (+15.4%) and PUFA-containing LPG (+9.4%) but decreased LPA plasma levels (−17.2%). Therefore, cold-induced

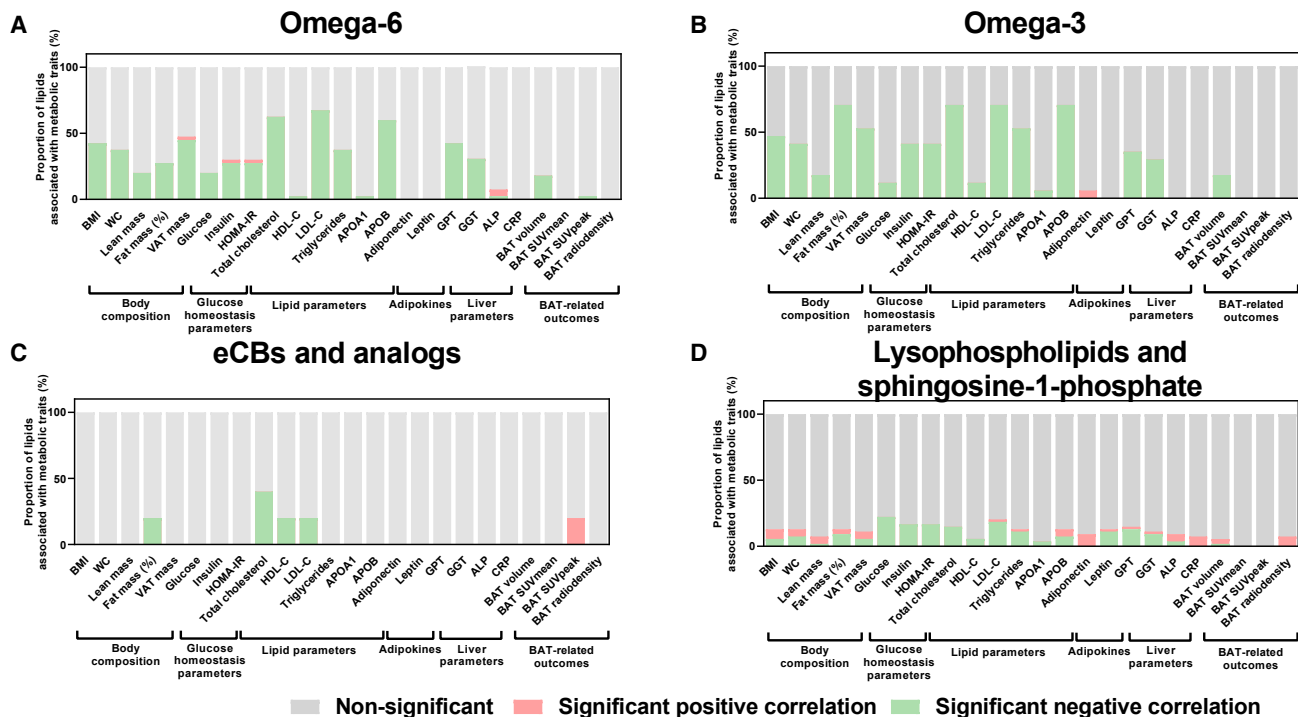


**Figure 4. Relationship of cold-induced changes on the plasma levels of signaling lipids with cardiometabolic risk factors and brown adipose tissue**

Bar graphs showing the proportion of cold-induced changes in omega-6 oxylipins (A), omega-3 oxylipins (B), endocannabinoids and analogs (eCBs, C), and lysophospholipids and sphingosine-1-phosphate (D) associated with cardiometabolic risk factors. Associations were determined by Pearson bivariate correlation analyses or partial correlation analyses (for brown adipose tissue). Partial correlation analyses were adjusted for the natural calendar day when the baseline PET/CT scan was performed. Cold-induced changes in plasma lipidome were determined by the 120-min fold change relative to baseline. Significance was set at  $p$  value  $< 0.05$  after FDR correction. Gray parts represent the proportion of lipids showing non-significant correlations, red parts represent the proportion of lipids showing significant positive correlations, whereas green parts represent the proportion of lipids showing significant negative correlations. Abbreviations are as follows: ALP, alkaline phosphatase; APOA1, apolipoprotein A1; APOB, apolipoprotein B; BAT, brown adipose tissue; BMI, body mass index; CRP, C-reactive protein; eCBs, endocannabinoids; GGT, gamma-glutamyl transferase; GPT, glutamic pyruvic transaminase; HDL-C, high-density lipoprotein cholesterol; HOMA-IR, homeostatic model assessment of insulin resistance index; LDL-C, low-density lipoprotein cholesterol; SUV, standardized uptake value; VAT, visceral adipose tissue; WC, waist circumference.

PUFA-containing LPE and LPG increased along with the increase in PUFAs and derived oxylipins. The physiological roles of LPE and LPG have not been fully elucidated, but they might be involved in membrane biosynthesis and inflammatory/immune signaling, specifically those containing PUFAs.<sup>44,45</sup> Contrarily, LPA is known to be a precursor for phosphatidic acid, which is required for the biosynthesis of triglycerides.<sup>46</sup> Recently, we demonstrated that cold exposure elicits an increase in PUFA-containing triglycerides,<sup>27</sup> which might partially tie in with our results. Overall, the physiological role of these cold-induced changes in plasma signaling lipids is still unknown. Future studies should include phospholipids precursors to fully understand their role upon acute cold exposure and to investigate whether changes in lysophospholipids are involved in the lipoprotein remodeling under cold stress or phospholipase activity.

#### Influence of brown adipose tissue in the cold-induced changes of the plasma signaling lipids

12,13-DiHOME, 12-HEPE, and MaR2 have been identified as brown fat lipokines.<sup>18–20</sup> Unfortunately, the liquid chromatog-

raphy-tandem mass spectrometry (LC-MS/MS) workflow used in this study did not detect 12-HEPE and MaR2 levels but detected 12,13-DiHOME. In a previous study, 1 h of cold exposure at 14°C increased 12,13-DiHOME plasma levels by ~1-fold in 9 healthy humans and was positively correlated with BAT activity measured by <sup>18</sup>F-FDG-PET/CT scan.<sup>18</sup> Serum and BAT levels of 12,13-DiHOME also increased in mice after 1 h of cold exposure at 4°C, and mice injected with 12,13-DiHOME increased BAT thermogenic activity.<sup>18</sup> Although we found that 12,13-DiHOME significantly increased in response to cold exposure ( $n = 64$ ; +39.4%), we found no correlation between the 12,13-DiHOME after cold exposure or at overnight fasting levels<sup>47</sup> with any BAT parameters (i.e., volume, SUVmean, SUVpeak, and radiodensity). Altogether, it suggests that human <sup>18</sup>F-FDG uptake by BAT is not responsible for the increase of this “brown fat lipokine” in response to cold exposure. Similarly, 5-HETE and 5,6-EpETrE were associated with the abundance of brown adipocytes in humans and mice.<sup>48</sup> However, cold-induced changes in 5-HETE were not associated with BAT volume or activity in our study, and our LC-MS/MS workflow did not detect 5,6-EpETrE.



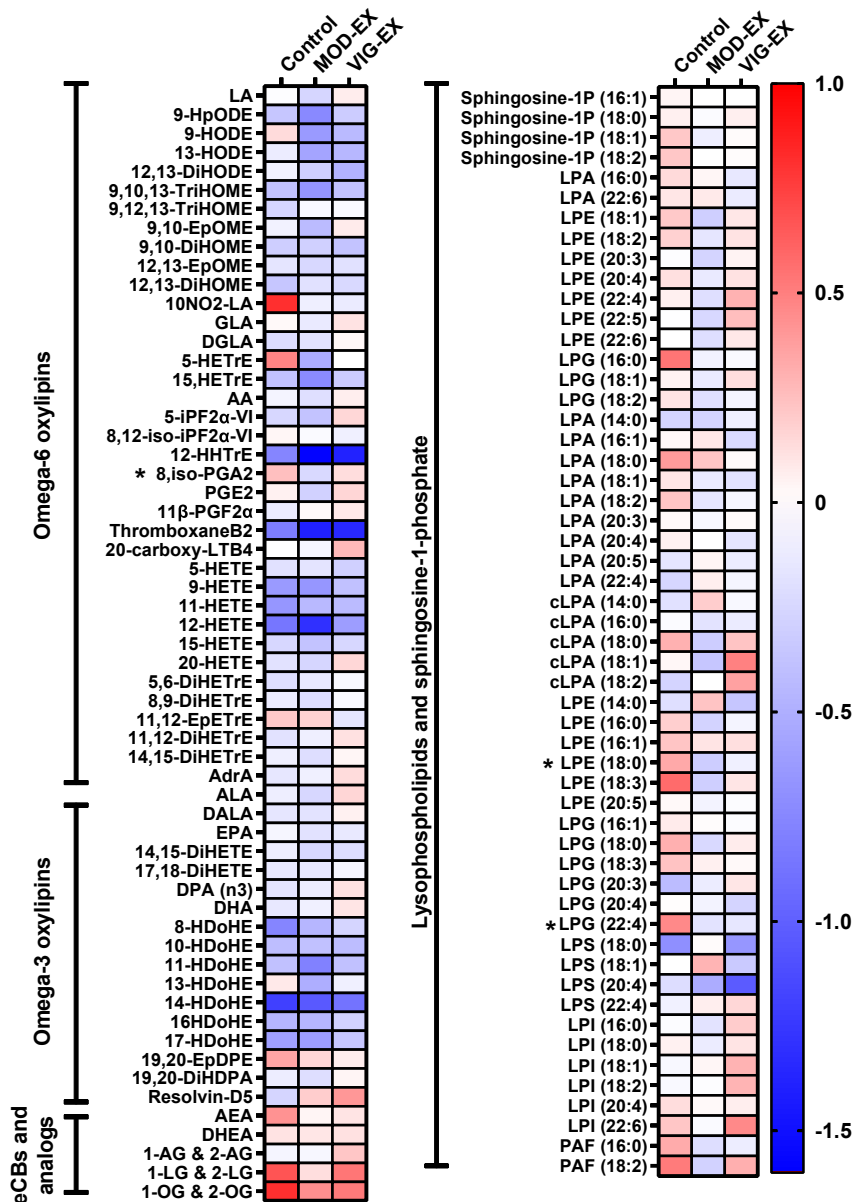


**Figure 5. Effect of 24-week supervised concurrent exercise intervention on the plasma levels of signaling lipids as a response to cold exposure**

Heatmap shows the changes in 120-min fold change after the intervention in each group. Each square represents the change after the intervention in 120-min fold change (i.e., post-intervention 120-min fold change minus pre-intervention 120-min fold change for each lipid). Blue squares represent a decrease, whereas red squares indicate an increase after the intervention. \*p value < 0.05, obtained from analyses of variance (ANOVA). The names and abbreviations of signaling lipids are detailed in Table S3. Abbreviations are as follows: CON, control group; MOD-EX, moderate-intensity exercise group; VIG-EX, vigorous-intensity exercise group.

relations between specific lipids (e.g., LA, GLA, and 5-HETrE) and BAT volume, and it is, therefore, unclear whether these correlations indicate a causal relationship. On the other hand, the positive correlation observed between cold-induced changes in 1-AG and 2-AG and BAT SUV<sub>peak</sub> is in line with previous evidence that acute cold exposure increased 2-AG levels in BAT of mice.<sup>22</sup> However, since no associations were observed with the rest of BAT parameters, further mechanistic studies are needed to be able to establish causality.

### Relationship of cold-induced changes in levels of oxylipins and cardiometabolic health

Our data also show that cold-induced changes in the levels of omega-6 and omega-3 oxylipins were related to the cardiometabolic traits (i.e., adiposity, glucose, lipid, and liver parameters). We recently observed that fasting plasma levels of omega-6 oxylipins were positively correlated to adiposity and cardiometabolic

Thus, future studies should investigate their potential relationship with human BAT in response to acute cold exposure.

In this study, we observed that cold exposure-induced changes in only 5% of the total lipid measured were weakly and negatively correlated with BAT volume. Since we did not observe these associations when we divided the cohort into men or women, normal-weight participants, or overweight and obese participants, our results should be interpreted cautiously. These results suggest that human BAT is not centrally involved in the cold-induced changes in the levels of signaling lipids and indicate that other tissues may be involved in the modulation and regulation of the cold-induced response in these lipids. Overall, the lack of association suggests that BAT may not produce these lipids in response to cold exposure and that BAT may not use those lipids as an energy source. However, the current study found moderate negative cor-

risk factors in young and middle-aged adults, whereas omega-3 oxylipins were negatively correlated.<sup>47,49</sup> Increased adiposity (i.e., obesity) and cardiometabolic diseases (e.g., type 2 diabetes and atherosclerosis) are characterized by chronic inflammation.<sup>50</sup> These diseases also disrupt the production of pro-inflammatory and anti-inflammatory/pro-resolution mediators in response to acute stressors (e.g., cold exposure and exercise).<sup>36</sup> Indeed, in our study cohort, participants with obesity showed higher overnight fasting levels of omega-6 oxylipins and lower fasting levels of omega-3 oxylipins than participants with normal weight.<sup>47</sup> In line with these findings, individuals overweight or obese displayed lower cold-induced increments in omega-6 and omega-3 oxylipins (+31.6% and +69.9%) than normal-weight participants (+58.0% and +81.9%). Interestingly, a large proportion (~45%) of cold-induced changes in the levels

of omega-6 and omega-3 oxylipins were associated with a healthier cardiometabolic profile (i.e., adiposity, glucose, lipid, and liver parameters) in the entire cohort. However, cold-induced changes in the levels of omega-6 and omega-3 oxylipins were not associated with adiposity, glucose homeostasis, or liver parameters in overweight or obese individuals. Therefore, our results suggest that individuals with higher adiposity and an unfavorable cardiometabolic profile have an impairment in releasing omega-6 (pro-inflammatory) and omega-3 (anti-inflammatory/pro-resolution) oxylipins to the circulation upon a 2-h cold exposure. These findings agree with previous results from our lab and suggest that oxylipins could potentially be considered cardiometabolic risk markers.<sup>47,49,51</sup> Obesity and cardiometabolic diseases are characterized by a systemic metabolic dysfunction involving impairments in adipose tissue, pancreas, liver, gut, or immune cells<sup>4,52</sup> and whole-body metabolic inflexibility.<sup>53</sup> Nevertheless, it remains unknown which tissues are the main contributors to the circulating levels of omega-6 and omega-3 oxylipins,<sup>54,55</sup> but it is plausible that BAT may not be responsible for the cold-induced changes in these metabolites in humans. Therefore, different organs (i.e., pancreas, liver, gut, or immune cells) might impair cold-induced omega-6 and omega-3 oxylipin production. The cold-induced increments in these lipids might be the normal physiological response, warranting further studies to elucidate their cold-induced changes in cardiometabolic-compromised populations and the tissues responsible for their increments.

### Impact of exercise on the cold-induced changes in the levels of signaling lipids

Exercise is undoubtedly an effective strategy to improve overall health, specifically cardiometabolic health.<sup>56,57</sup> Interestingly, in a previous study, acute endurance exercise increased 12,13-DiHOME levels in active young and older male subjects (n = 27) and sedentary young adults (n = 12; 50% women).<sup>17</sup> 12,13-DiHOME levels also increased after acute and chronic (3 weeks) endurance exercise in mice, being secreted from BAT in response to exercise.<sup>17</sup> In contrast, in the present study, we observed that a 24-week supervised concurrent exercise intervention, which improved the cardiometabolic phenotype (e.g., adiposity and fitness<sup>25</sup>) and decreased fasting plasma levels of omega-6 oxylipins (including 12,13-DiHOME) and eCBs,<sup>26</sup> did not modify plasma signaling lipid response to cold exposure. Additionally, we found no association between the changes in the levels of signaling lipids and BAT changes, suggesting that BAT may not be involved in regulating these lipids in response to cold exposure.

### Limitations of the study

A significant strength is the inclusion of men, women, individuals with normal weight, and participants overweight or obese. Another strength is the metabolomics-based methodology targeting omega-6 and omega-3 oxylipins, eCBs and analogs, lysophospholipids, and sphingosine-1-phosphate. Nevertheless, the short time of the cold exposure does not allow us to extrapolate our results to longer or milder/cooler cold interventions. Our study lacks a thermoneutral PET/CT scan as a reference. Additionally, the current method used for quantifying BAT volume

and activity has several limitations,<sup>58</sup> which suggests that the data should be interpreted cautiously. Future studies using different methodologies and radiotracers are required to address the influence of BAT in the cold-induced changes of the signaling lipids in humans. Moreover, the inclusion of young adults does not allow for extrapolation of the findings to older populations, children, or individuals with metabolic abnormalities. Lastly, the relatively low sample size when dividing the cohort by gender or BMI and in the exercise intervention might dampen the generalizability of the findings.

### Conclusions

2-h cold exposure influences plasma signaling lipids (i.e., omega-6 and omega-3 oxylipins, endocannabinoids, lysophospholipids, and sphingosine-1-phosphate species) in young adults. Cold-induced changes in omega-6 and omega-3 oxylipins are related to a healthier cardiometabolic profile but not to BAT parameters (i.e., volume, activity, and radiodensity). Finally, the observed cold-induced changes in plasma signaling lipids are not modified after a 24-week exercise intervention in young adults. Further studies are needed to understand the role of cold exposure and exercise in modulating these metabolites and the role of cold-induced changes on cardiometabolic health.

### STAR★METHODS

Detailed methods are provided in the online version of this paper and include the following:

- KEY RESOURCES TABLE
- RESOURCES AVAILABILITY
  - Lead contact
  - Materials availability
  - Data and code availability
- EXPERIMENTAL MODEL AND STUDY PARTICIPANTS DETAILS
  - Participants
  - Study design
- METHODS DETAILS
  - Cold exposure and <sup>18</sup>F-fluorodeoxyglucose uptake by brown adipose tissue
  - Long-term exercise intervention
  - Blood sample collection
  - Determination of plasma signaling lipids
  - Anthropometric and body composition
  - Cardiometabolic risk factors
- QUANTIFICATION AND STATISTICAL ANALYSIS
- ADDITIONAL RESOURCES

### SUPPLEMENTAL INFORMATION

Supplemental information can be found online at <https://doi.org/10.1016/j.xcrm.2023.101387>.

### ACKNOWLEDGMENTS

The authors would like to thank all the participants of this study for their time and effort. This study is part of a Ph.D. thesis conducted in the Biomedicine Doctoral Studies of the University of Granada, Spain.

The study was supported by the Junta de Andalucía, Consejería de Transformación Económica, Industria, Conocimiento y Universidades Dirección General de Investigación y Transferencia del Conocimiento (ref. P18-RT-4455, ref. SOMM17/6107/UGR, and DOC 01151) and European Regional Development Funds (ERDF), the Spanish Ministry of Economy and Competitiveness via the Fondo de Investigación Sanitaria del Instituto de Salud Carlos III (PI13/01393), and PTA-12264, Retos de la Sociedad (DEP2016-79512-R), the Spanish Ministry of Education (FPU19/01609), the Fundación Iberoamericana de Nutrición (FINUT), the Redes Temáticas de Investigación Cooperativa RETIC (Red SAMID RD16/0022), the AstraZeneca HealthCare Foundation, the University of Granada Plan Propio de Investigación 2016 Excellence actions: Unit of Excellence on Exercise and Health (UCEES), and the Chinese Scholarship Council fellowships (no. 201707060012 for X.D. and no. 201607060017 for W.Y.). B.M.T. is supported by a grant for the requalification of the Spanish university system from the Ministry of Universities of the Government of Spain, financed by the European Union, NextGeneration EU (María Zambrano program, reference RR\_C\_2021\_04).

#### AUTHOR CONTRIBUTIONS

Conceptualization, L.J.-F., G.S.-D., J.R.R., and B.M.-T.; methodology, L.J.-F., G.S.-D., F.V., C.M.A., J.R.R., and B.M.-T.; validation, X.D., W.Y., T.H., I.K., C.M.A., and F.V.; formal analysis, L.J.-F., G.S.-D., and B.M.-T.; data collection, G.S.-D., X.D., W.Y., T.H., and I.K.; data curation, L.J.-F. and B.M.-T.; writing – original draft, L.J.-F., J.R.R., and B.M.-T.; writing – review and editing, all authors; supervision, J.R.R. and B.M.-T. All authors commented on the manuscript and approved the final version of the manuscript.

#### DECLARATION OF INTERESTS

The authors declare no competing interests.

Received: June 21, 2023

Revised: September 27, 2023

Accepted: December 22, 2023

Published: January 22, 2024

#### REFERENCES

- Vedanthan, R., and Fuster, V. (2011). Urgent need for human resources to promote global cardiovascular health. *Preprint. Nat. Rev. Cardiol.* *8*, 114–117.
- Organization, W.H. Cardiovascular Diseases (CVDs).
- WHO (2018). Noncommunicable Diseases Country Profiles 2018.
- Blüher, M. (2019). Obesity: Global Epidemiology and Pathogenesis (Preprint at Nature Publishing Group).
- Ruiz, J.R., Martínez-Tellez, B., Sánchez-Delgado, G., Osuna-Prieto, F.J., Rensen, P.C.N., and Boon, M.R. (2018). Role of Human Brown Fat in Obesity, Metabolism and Cardiovascular Disease: Strategies to Turn Up the Heat. *Prog. Cardiovasc. Dis.* *61*, 232–245.
- Schrauwen, P., and van Marken Lichtenbelt, W.D. (2016). Combatting Type 2 Diabetes by Turning up the Heat (Preprint at Springer Verlag).
- Hanssen, M.J.W., Hoeks, J., Brans, B., van der Lans, A.A.J.J., Schaart, G., van den Driessche, J.J., Jörgensen, J.A., Boekschoten, M.v., Hesselink, M.K.C., Havekes, B., et al. (2015). Short-term cold acclimation improves insulin sensitivity in patients with type 2 diabetes mellitus. *Nat. Med.* *21*, 863–865.
- De Lorenzo, F., Mukherjee, M., Kadziola, Z., Sherwood, R., and Kakkar, V. (1998). Central cooling effects in patients with hypercholesterolaemia. *Clin. Sci.* *95*, 213–217.
- Ivanova, Y.M., and Blondin, D.P. (2021). Examining the benefits of cold exposure as a therapeutic strategy for obesity and type 2 diabetes. *J. Appl. Physiol.* *130*, 1448–1459.
- Cannon, B., and Nedergaard, J. (2004). Brown adipose tissue: function and physiological significance. *Physiol. Rev.* *84*, 277–359.

- Scheele, C. (2021). Perspectives on the role of brown adipose tissue in human body temperature and metabolism. *Cell Rep. Med.* *2*, 100427.
- Søberg, S., Löfgren, J., Philipsen, F.E., Jensen, M., Hansen, A.E., Ahrens, E., Nystrup, K.B., Nielsen, R.D., Sølling, C., Wedell-Neergaard, A.-S., et al. (2021). Altered brown fat thermoregulation and enhanced cold-induced thermogenesis in young, healthy, winter-swimming men. *Cell Rep. Med.* *2*, 100408.
- Becher, T., Palanisamy, S., Kramer, D.J., Eljalby, M., Marx, S.J., Wibmer, A.G., Butler, S.D., Jiang, C.S., Vaughan, R., Schöder, H., et al. (2021). Brown adipose tissue is associated with cardiometabolic health. *Nat. Med.* *27*, 58–65.
- Villarroya, F., Cereijo, R., Villarroya, J., and Giralt, M. (2017). Brown adipose tissue as a secretory organ. *Nat. Rev. Endocrinol.* *13*, 26–35.
- Scheele, C., and Wolfrum, C. (2020). Brown adipose crosstalk in tissue plasticity and human metabolism. *Endocr. Rev.* *41*, 53–65.
- Deshmukh, A.S., Peijs, L., Beaudry, J.L., Jespersen, N.Z., Nielsen, C.H., Ma, T., Brunner, A.D., Larsen, T.J., Bayarri-Olmos, R., Prabhakar, B.S., et al. (2019). Proteomics-based comparative mapping of the secretomes of human brown and white adipocytes reveals EPDR1 as a novel batokine. *Cell Metab.* *30*, 963–975.e7.
- Stanford, K.I., Lynes, M.D., Takahashi, H., Baer, L.A., Arts, P.J., May, F.J., Lehnig, A.C., Middelbeek, R.J.W., Richard, J.J., So, K., et al. (2018). 12,13-diHOME: An Exercise-Induced Lipokine that Increases Skeletal Muscle Fatty Acid Uptake. *Cell Metab.* *27*, 1111–1120.e3.
- Lynes, M.D., Leiria, L.O., Lundh, M., Bartelt, A., Shamsi, F., Huang, T.L., Takahashi, H., Hirshman, M.F., Schlein, C., Lee, A., et al. (2017). The cold-induced lipokine 12,13-diHOME promotes fatty acid transport into brown adipose tissue. *Nat. Med.* *23*, 631–637.
- Leiria, L.O., Wang, C.H., Lynes, M.D., Yang, K., Shamsi, F., Sato, M., Sugimoto, S., Chen, E.Y., Bussberg, V., Narain, N.R., et al. (2019). 12-Lipoxygenase Regulates Cold Adaptation and Glucose Metabolism by Producing the Omega-3 Lipid 12-HEPE from Brown Fat. *Cell Metab.* *30*, 768–783.e7.
- Sugimoto, S., Mena, H.A., Sansbury, B.E., Kobayashi, S., Tsuji, T., Wang, C.-H., Yin, X., Huang, T.L., Kusuyama, J., Kodani, S.D., et al. (2022). Brown adipose tissue-derived MaR2 contributes to cold-induced resolution of inflammation. *Nat. Metab.* *4*, 775–790.
- van Eenige, R., van der Stelt, M., Rensen, P.C.N., and Kooijman, S. (2018). Regulation of Adipose Tissue Metabolism by the Endocannabinoid System (Preprint at Elsevier Inc).
- Krott, L.M., Piscitelli, F., Heine, M., Borrino, S., Scheja, L., Silvestri, C., Heeren, J., and Di Marzo, V. (2016). Endocannabinoid regulation in white and brown adipose tissue following thermogenic activation. *J. Lipid Res.* *57*, 464–473.
- Pernes, G., Morgan, P.K., Huynh, K., Mellett, N.A., Meikle, P.J., Murphy, A.J., Henstridge, D.C., and Lancaster, G.I. (2021). Characterization of the circulating and tissue-specific alterations to the lipidome in response to moderate and major cold stress in mice. *Am. J. Physiol. Regul. Integr. Comp. Physiol.* *320*, R95–R104.
- Ruiz, J.R., Martínez-Tellez, B., Sánchez-Delgado, G., Aguilera, C.M., and Gil, A. (2015). Regulation of Energy Balance by Brown Adipose Tissue: At Least Three Potential Roles for Physical Activity (Preprint at BMJ Publishing Group Ltd and British Association of Sport and Exercise Medicine).
- Martínez-Tellez, B., Sánchez-Delgado, G., Acosta, F.M., Alcantara, J.M.A., Amaro-Gahete, F.J., Martínez-Avila, W.D., Merchan-Ramírez, E., Muñoz-Hernández, V., Osuna-Prieto, F.J., Jurado-Fasoli, L., et al. (2022). No evidence of brown adipose tissue activation after 24 weeks of supervised exercise training in young sedentary adults in the ACTIBATE randomized controlled trial. *Nat. Commun.* *13*, 5259.
- Jurado-Fasoli, L., Di, X., Sánchez-Delgado, G., Yang, W., Osuna-Prieto, F.J., Ortiz-Alvarez, L., Kerkels, E., Harms, A.C., Hankemeier, T., Schönke, M., et al. (2022). Acute and long-term exercise differently modulate plasma levels of oxylipins, endocannabinoids, and their analogues in young

- sedentary adults: A sub-study and secondary analyses from the ACTIBATE randomized controlled-trial. *EBioMedicine* 85, 104313.
27. Straat, M.E., Jurado-Fasoli, L., Ying, Z., Nahon, K.J., Janssen, L.G.M., Boon, M.R., Grabner, G.F., Kooijman, S., Zimmermann, R., Giera, M., et al. (2022). Cold exposure induces dynamic changes in circulating triacylglycerol species, which is dependent on intracellular lipolysis: A randomized cross-over trial. *EBioMedicine* 86, 104349.
  28. Straat, M.E., Martinez-Tellez, B., Janssen, L.G.M., van Veen, S., van Eenige, R., Kharagjitsing, A.v., van den Berg, S.A.A., de Rijke, Y.B., Haks, M.C., Rensen, P.C.N., and Boon, M.R. (2022). The effect of cold exposure on circulating transcript levels of immune genes in Dutch South Asian and Dutch European men. *J. Therm. Biol.* 107, 103259.
  29. Brenner, I.K.M., Castellani, J.W., Gabaree, C., Young, A.J., Zamecnik, J., Shephard, R.J., Shek, A.P.N., and Shek, P.N. Immune changes in humans during cold exposure: effects of prior heating and exercise.
  30. Gagnon, D.D., Gagnon, S.S., Rintamäki, H., Törmäkangas, T., Puukka, K., Herzig, K.H., and Kyröläinen, H. (2014). The effects of cold exposure on leukocytes, hormones and cytokines during acute exercise in humans. *PLoS One* 9, e110774.
  31. Dyall, S.C., Balas, L., Bazan, N.G., Brenna, J.T., Chiang, N., da Costa Souza, F., Dall'Aglio, J., Durand, T., Galano, J.-M., Lein, P.J., et al. (2022). Polyunsaturated fatty acids and fatty acid-derived lipid mediators: Recent advances in the understanding of their biosynthesis, structures, and functions. *Prog. Lipid Res.* 86, 101165.
  32. Zidar, N., Odar, K., Glavac, D., Jerse, M., Zupanc, T., and Stajner, D. (2009). Cyclooxygenase in normal human tissues - is COX-1 really a constitutive isoform, and COX-2 an inducible isoform? *J. Cell Mol. Med.* 13, 3753–3763.
  33. Ni, K.D., and Liu, J.Y. (2021). The Functions of Cytochrome P450  $\omega$ -hydroxylases and the Associated Eicosanoids in Inflammation-Related Diseases. *Front. Pharmacol.* 12, 716801.
  34. Bishop-Bailey, D., Thomson, S., Askari, A., Faulkner, A., and Wheeler-Jones, C. (2014). Lipid-metabolizing CYPs in the regulation and dysregulation of metabolism. *Annu. Rev. Nutr.* 34, 261–279.
  35. Bannenberg, G., and Serhan, C.N. (2010). Specialized pro-resolving lipid mediators in the inflammatory response: An update. *Biochim. Biophys. Acta* 1807, 1260–1273.
  36. Spite, M., Clària, J., and Serhan, C.N. (2014). Resolvins, specialized pro-resolving lipid mediators, and their potential roles in metabolic diseases. *Cell Metab.* 19, 21–36.
  37. Serhan, C.N., Chiang, N., and van Dyke, T.E. (2008). Resolving inflammation: Dual anti-inflammatory and pro-resolution lipid mediators. *Nat. Rev. Immunol.* 8, 349–361.
  38. Chen, L., Yan, G., and Ohwada, T. (2022). Building on Endogenous Lipid Mediators to Design Synthetic Receptor Ligands (Preprint at Elsevier Masson s.r.l.).
  39. Rahman, S.K., Uyama, T., Hussain, Z., and Ueda, N. (2021). Roles of Endocannabinoids and Endocannabinoid-like Molecules in Energy Homeostasis and Metabolic Regulation: A Nutritional Perspective. *Annu. Rev. Nutr.* 41, 177–202.
  40. McDougale, D.R., Watson, J.E., Abdeen, A.A., Adili, R., Caputo, M.P., Krapf, J.E., Johnson, R.W., Kilian, K.A., Holinstat, M., and Das, A. (2017). Anti-inflammatory  $\omega$ -3 endocannabinoid epoxides. *Proc. Natl. Acad. Sci. USA* 114, E6034–E6043.
  41. Lahesmaa, M., Eriksson, O., Gnad, T., Oikonen, V., Bucci, M., Hirvonen, J., Koskensalo, K., Teuhho, J., Niemi, T., Taittonen, M., et al. (2018). Cannabinoid type 1 receptors are upregulated during acute activation of brown adipose tissue. *Diabetes* 67, 1226–1236.
  42. Yang, M., Qi, X., Li, N., Kaifi, J.T., Chen, S., Wheeler, A.A., Kimchi, E.T., Ericsson, A.C., Rector, R.S., Staveley-O'Carroll, K.F., and Li, G. (2023). Western diet contributes to the pathogenesis of non-alcoholic steatohepatitis in male mice via remodeling gut microbiota and increasing production of 2-oleoylglycerol. *Nat. Commun.* 14, 228.
  43. Browning, K.N., and Travagli, R.A. (2014). Central nervous system control of gastrointestinal motility and secretion and modulation of gastrointestinal functions. *Compr. Physiol.* 4, 1339–1368.
  44. Tan, S.T., Ramesh, T., Toh, X.R., and Nguyen, L.N. (2020). Emerging Roles of Lysophospholipids in Health and Disease (Preprint at Elsevier Ltd).
  45. Ménégaut, L., Jalil, A., Thomas, C., and Masson, D. (2019). Macrophage Fatty Acid Metabolism and Atherosclerosis: The Rise of PUFAs (Preprint at Elsevier Ireland Ltd).
  46. Gimeno, R.E., and Cao, J. (2008). Mammalian glycerol-3-phosphate acyltransferases: New genes for an old activity. *J. Lipid Res.* 49, 2079–2088.
  47. Jurado-Fasoli, L., Di, X., Kohler, I., Osuna-Prieto, F.J., Hankemeier, T., Krekels, E., Harms, A.C., Yang, W., Garcia-Lario, J.v., Fernández-Veledo, S., et al. (2022). Omega-6 and omega-3 oxylipins as potential markers of cardiometabolic risk in young adults. *Obesity* 30, 50–61.
  48. Dieckmann, S., Maurer, S., Fromme, T., Colson, C., Virtanen, K.A., Amri, E.Z., and Klingenspor, M. (2020). Fatty Acid Metabolite Profiling Reveals Oxylipins as Markers of Brown but Not Brite Adipose Tissue. *Front. Endocrinol.* 11, 73.
  49. Jurado-Fasoli, L., Osuna-Prieto, F.J., Yang, W., Kohler, I., Di, X., Rensen, P.C.N., Castillo, M.J., Martinez-Tellez, B., and Amaro-Gahete, F.J. (2023). High omega-6/omega-3 fatty acid and oxylipin ratio in plasma is linked to an adverse cardiometabolic profile in middle-aged adults. *J. Nutr. Biochem.* 117, 109331.
  50. Hotamisligil, G.S. (2006). Inflammation and metabolic disorders. *Nature* 444, 860–867.
  51. Osuna-Prieto, F.J., Martinez-Tellez, B., Ortiz-Alvarez, L., Di, X., Jurado-Fasoli, L., Xu, H., Ceperuelo-Mallafre, V., Núñez-Roa, C., Kohler, I., Segura-Carretero, A., et al. (2021). Elevated plasma succinate levels are linked to higher cardiovascular disease risk factors in young adults. *Cardiovasc. Diabetol.* 20, 151.
  52. Reilly, S.M., and Saltiel, A.R. (2017). Adapting to obesity with adipose tissue inflammation. *Nat. Rev. Endocrinol.* 13, 633–643.
  53. Amaro-Gahete, F.J., Sanchez-Delgado, G., Ara, I., and R Ruiz, J. (2019). Cardiorespiratory fitness may influence metabolic inflexibility during exercise in obese persons. *J. Clin. Endocrinol. Metab.* 104, 5780–5790.
  54. Gabbs, M., Leng, S., Devassy, J.G., Monirujjaman, M., and Aukema, H.M. (2015). Advances in Our Understanding of Oxylipins Derived from Dietary PUFAs. *Adv. Nutr.* 6, 513–540.
  55. Nieman, D.C., Lila, M.A., and Gillitt, N.D. (2019). Immunometabolism: A Multi-Omics Approach to Interpreting the Influence of Exercise and Diet on the Immune System. *Annu. Rev. Food Sci. Technol.* 10, 341–363.
  56. Bellicha, A., van Baak, M.A., Battista, F., Beaulieu, K., Blundell, J.E., Busetto, L., Carraça, E.V., Dicker, D., Encantado, J., Ermolao, A., et al. (2021). Effect of exercise training on weight loss, body composition changes, and weight maintenance in adults with overweight or obesity: An overview of 12 systematic reviews and 149 studies. *Obes. Rev.* 22, e13256.
  57. Battista, F., Ermolao, A., van Baak, M.A., Beaulieu, K., Blundell, J.E., Busetto, L., Carraça, E.V., Encantado, J., Dicker, D., Farpour-Lambert, N., et al. (2021). Effect of exercise on cardiometabolic health of adults with overweight or obesity: Focus on blood pressure, insulin resistance, and intrahepatic fat—A systematic review and meta-analysis. *Obes. Rev.* 22, e13269.
  58. Carpentier, A.C., Blondin, D.P., Virtanen, K.A., Richard, D., Haman, F., and Turcotte, É.E. (2018). Brown adipose tissue energy metabolism in humans. *Front. Endocrinol.* 9, 447.
  59. Sanchez-Delgado, G., Martinez-Tellez, B., Olza, J., Aguilera, C.M., Labayen, I., Ortega, F.B., Chillón, P., Fernandez-Reguera, C., Alcantara, J.M.A., Martinez-Avila, W.D., et al. (2015). Activating brown adipose tissue through exercise (ACTIBATE) in young adults: Rationale, design and methodology. *Contemp. Clin. Trials* 45, 416–425.

60. Schulz, K.F., Grimes, D.A., Schulz, K.F., and Grimes, D.A. (2002). Generation of allocation sequences in randomised trials: chance, not choice. *Lancet* 359, 515–519.
61. Friedberg, J.P., Lipsitz, S.R., and Natarajan, S. (2010). Challenges and recommendations for blinding in behavioral interventions illustrated using a case study of a behavioral intervention to lower blood pressure. Preprint 78, 5–11.
62. Martínez-Tellez, B., Sánchez-Delgado, G., García-Rivero, Y., Alcántara, J.M.A., Martínez-Avila, W.D., Muñoz-Hernández, M.V., Olza, J., Boon, M.R., Rensen, P.C.N., Llamas-Elvira, J.M., and Ruiz, J.R. (2017). A new personalized cooling protocol to activate brown adipose tissue in young adults. *Front. Physiol.* 8, 863.
63. Cypess, A.M., Lehman, S., Williams, G., Tal, I., Rodman, D., Goldfine, A.B., Kuo, F.C., Palmer, E.L., Tseng, Y.-H., Doria, A., et al. (2009). Identification and importance of brown adipose tissue in adult humans. *N. Engl. J. Med.* 360, 1509–1517.
64. Schindelin, J., Arganda-Carreras, I., Frise, E., Kaynig, V., Longair, M., Pietzsch, T., Preibisch, S., Rueden, C., Saalfeld, S., Schmid, B., et al. (2012). Fiji: an open-source platform for biological-image analysis. *Nat. Methods* 9, 676–682.
65. Chen, K.Y., Cypess, A.M., Laughlin, M.R., Haft, C.R., Hu, H.H., Bredella, M.A., Enerbäck, S., Kinahan, P.E., Lichtenbelt, W.v.M., Lin, F.I., et al. (2016). Brown Adipose Reporting Criteria in Imaging Studies (BARCIST 1.0): Recommendations for Standardized FDG-PET/CT Experiments in Humans. *Cell Metab.* 24, 210–222.
66. Martínez-Tellez, B., Sánchez-Delgado, G., Boon, M.R., Rensen, P.C.N., Llamas-Elvira, J.M., and Ruiz, J.R. (2019). Distribution of Brown Adipose Tissue Radiodensity in Young Adults: Implications for Cold [18F]FDG-PET/CT Analyses. *Mol. Imag. Biol.* 22, 425–433.
67. Martínez-Tellez, B., Nahon, K.J., Sánchez-Delgado, G., Abreu-Vieira, G., Llamas-Elvira, J.M., van Velden, F.H.P., Pereira Arias-Bouda, L.M., Rensen, P.C.N., Boon, M.R., and Ruiz, J.R. (2018). The impact of using BARCIST 1.0 criteria on quantification of BAT volume and activity in three independent cohorts of adults. *Sci. Rep.* 8, 8567.
68. Jurado-Fasoli, L., Yang, W., Kohler, I., Dote-Montero, M., Osuna-Prieto, F.J., Di, X., Hankemeier, T., Krekels, E.H., Harms, A.C., Castillo, M.J., et al. (2022). Effect of Different Exercise Training Modalities on Fasting Levels of Oxylipins and Endocannabinoids in Middle-Aged Sedentary Adults: A Randomized Controlled Trial. *Int. J. Sport Nutr. Exerc. Metab.* 32, 275–284.
69. di Zazzo, A., Yang, W., Coassin, M., Micera, A., Antonini, M., Piccinni, F., de Piano, M., Kohler, I., Harms, A.C., Hankemeier, T., et al. (2020). Signaling lipids as diagnostic biomarkers for ocular surface cicatrizing conjunctivitis. *J. Mol. Med.* 98, 751–760.
70. Van Der Kloet, F.M., Bobeldijk, I., Verheij, E.R., and Jellema, R.H. (2009). Analytical error reduction using single point calibration for accurate and precise metabolomic phenotyping. *J. Proteome Res.* 8, 5132–5141.
71. Matthews, J.C. (1985). Instability of brain synaptosomal membrane preparations to repeated ultracentrifugation in isoosmotic density gradients. *Life Sci.* 37, 2467–2473.
72. Benjamini, Y., and Hochberg, Y. (1995). Controlling the False Discovery Rate : A Practical and Powerful Approach to Multiple Testing. *J. Roy. Stat. Soc.* 57, 289–300.

STAR★METHODS

KEY RESOURCES TABLE

REAGENT or RESOURCE	SOURCE	IDENTIFIER
<b>Biological samples</b>		
Human plasma and serum samples	Clinical Trial	NCT-02365129
<b>Critical commercial assays</b>		
Glucose assay kit	Beckman Coulter	#OSR6521
Insulin assay kit	Beckman Coulter	#OSR33410
Cholesterol assay kit	Beckman Coulter	#OSR6516
HDL-C assay kit	Beckman Coulter	#OSR6587
Triacylglycerols assay kit	Beckman Coulter	#OSR61118
APOA1	Beckman Coulter	446410
APOB	Beckman Coulter	447730
GGT assay kit	Beckman Coulter	#OSR6507
ALT assay kit	Beckman Coulter	#OSR6507
ALP assay kit	Beckman Coulter	#OSR6204
CRP assay kit	Beckman Coulter	#OSR6299
Leptin MILLIPLEX MAG Human Adipokine Magnetic Bead Panel	Luminex Corporation	# HADK2MAG-61K
Adiponectin MILLIPLEX MAP Human Adipokine Magnetic Bead Panel 1	Luminex Corporation	Catalog # HADK1MAG-61K
<b>Deposited data</b>		
Lipidomic data	This paper	Metabolights: MTBLS9035
<b>Software and algorithms</b>		
Fiji- ImageJ	Fiji software	<a href="https://sourceforge.net/p/bijijiplugins/wiki/Brown%20fat%20Volume/">https://sourceforge.net/p/bijijiplugins/wiki/Brown%20fat%20Volume/</a>
Statistical Package for the Social Sciences v.27.0	IBM Corporation	<a href="https://www.ibm.com/analytics/spss-statistics-software">https://www.ibm.com/analytics/spss-statistics-software</a> . RRID:SCR_002865
R v.4.1.2	CRAN	<a href="https://cran.r-project.org/">https://cran.r-project.org/</a>
GraphPad Prism v.9	GraphPad Software	<a href="http://www.graphpad.com/RRID:SCR_002798">http://www.graphpad.com/RRID: SCR_002798</a>
SCIEX OS-MQ Software	SCIEX	<a href="https://sciex.com/products/software/sciex-os-software">https://sciex.com/products/software/sciex-os-software</a>
mzQuality workflow	mzQuality	<a href="http://www.mzQuality.nl">http://www.mzQuality.nl</a>
<b>Other</b>		
<sup>18</sup> F-FDG-Radiotracer	IBA molecular	N/A
Dual X-ray absorptiometry (DXA)	Hologic Discovery	<a href="https://medpick.in/product/hologic-discovery-wi-bone-densitometers/">https://medpick.in/product/hologic-discovery-wi-bone-densitometers/</a>
Cooling vests and chillers	Polar Products Inc.	<a href="https://www.polarproducts.com/polarshop/pc/Cooling-Systems-for-Operating-Rooms-and-Medical-Facilities-c444.htm">https://www.polarproducts.com/polarshop/pc/Cooling-Systems-for-Operating-Rooms-and-Medical-Facilities-c444.htm</a>
16 PET/CT scanner	Siemens Biograph	<a href="https://www.siemens-healthineers.com/nl/molecular-imaging/pet-ct/biograph-vision">https://www.siemens-healthineers.com/nl/molecular-imaging/pet-ct/biograph-vision</a>
LC system	Shimadzu LC system	<a href="https://www.shimadzu.com/an/products/liquid-chromatography/index.html">https://www.shimadzu.com/an/products/liquid-chromatography/index.html</a>
Mass spectrometer	SCIEX QTRAP 7500+	<a href="https://sciex.com/products/mass-spectrometers/triple-quad-systems/triple-quad-7500-system">https://sciex.com/products/mass-spectrometers/triple-quad-systems/triple-quad-7500-system</a>
LCMS system	Shimadzu LCMS-8060 system	<a href="https://www.shimadzu.com/an/products/liquid-chromatograph-mass-spectrometry/triple-quadrupole-lc-msms/lcms-8060/index.html">https://www.shimadzu.com/an/products/liquid-chromatograph-mass-spectrometry/triple-quadrupole-lc-msms/lcms-8060/index.html</a>

## RESOURCES AVAILABILITY

### Lead contact

Further information and requests for resources and reagents should be directed to and will be fulfilled by the Lead Contact, Dr. Jonathan R. Ruiz ([ruizj@ugr.es](mailto:ruizj@ugr.es)).

### Materials availability

The study did not generate new unique reagents.

### Data and code availability

- The lipidomic data of this study have been recorded at Metabolights: MTBLS9035. Data are available from the [lead contact](#) upon request and with the permission of the Research Data Deposit Management Committee.
- This paper does not report original code.
- Any additional information required to reanalyze the data reported in this paper is available from the [lead contact](#) upon request

## EXPERIMENTAL MODEL AND STUDY PARTICIPANTS DETAILS

### Participants

This study was conducted under the framework of the ACTIBATE (*ACTivating Brown Adipose Tissue through Exercise*; [ClinicalTrials.gov](#) ID: NCT02365129; [Figure 1](#)) randomized controlled trial,<sup>59</sup> of which the detailed study design is described elsewhere<sup>25,59</sup> and follows the STROBE ([Table S1](#)) CONSORT guidelines ([Table S2](#)). The ACTIBATE study included 145 young sedentary adults aged between 18 and 25 years. Participants were recruited through social networks, local media, and posters in Granada (Spain). Inclusion criteria included reporting to be sedentary (i.e., <20 min/day of moderate-to-vigorous physical activity on <3 days/week), being a non-smoker, having stable body weight over the last three months, and not taking any medication. Exclusion criteria included being diagnosed with diabetes, hypertension, or other significant medical conditions that might interfere with or be aggravated by exercise, being pregnant, using medication deemed to affect energy metabolism, or being frequently exposed to cold temperatures.

### Study design

This work includes secondary analyses from the ACTIBATE study. The study was approved by the Ethics Committee on Human Research of the University of Granada (no. 924) and the *Servicio Andaluz de Salud (Centro de Granada, CEI-Granada, Spain)*. All participants provided informed consent. The study protocol and experimental design were applied following the last revised ethical guidelines of the Declaration of Helsinki. The study was carried out at the Sport and Health University Research Institute and the Virgen de las Nieves University Hospital of the University of Granada. The study was conducted over two consecutive years in four different waves per year (i.e., from September 2015 to June 2016 and from September 2016 to June 2017) and ended when the exercise intervention finished.

During baseline examinations, participants performed a 2 h cold exposure test. Blood samples were collected in a subgroup of participants ( $n = 64$ ;  $n = 47$  women) to investigate the effect of the cold exposure on the plasma signaling lipids (i.e., omega-6 and omega-3 oxylipins, eCBs and analogs, lysophospholipids, and sphingosine-1-phosphate species), just before BAT quantification. After baseline examinations, all participants were randomly assigned into three groups using computer-generated simple (unrestricted) randomization by the principal investigator,<sup>60</sup> namely, (i) control group (no exercise), (ii) moderate-intensity exercise group (MOD-EX), and (iii) vigorous-intensity exercise group (VIG-EX) ([Figure S1](#)). The randomization was unblinded and performed by JRR using an in-house system; no additional researcher had access. Participants were explicitly informed about the group to which they were assigned. No delay was experimented between randomization and the initiation of the intervention. Rigorous standardization procedures for data collection and intervention were followed to ensure the internal and external validity of the trial.<sup>61</sup> After the long-term exercise intervention, participants performed an additional 2 h cold exposure test ([Figure S1](#)).

All participants were instructed not to change their daily routine, physical activity, or dietary patterns over the study period. No essential changes were performed in the methodology or outcomes after the beginning of the trial and no relevant adverse events were recorded.

## METHODS DETAILS

### Cold exposure and <sup>18</sup>F-fluorodeoxyglucose uptake by brown adipose tissue

Before the cold exposure test and BAT assessment, the shivering threshold of each participant was determined following an incremental cooling protocol<sup>62</sup> The procedure began in a warm room (22°C–23°C) where participants waited 30–45 min before entering a mild-cold room (19.5–20.0°C). Participants were then asked to wear a water-perfused cooling vest (Polar Products Inc., Stow, OH, USA), and the water temperature was progressively reduced until 3.8°C or until the first signs of shivering. If shivering did not occur, participants remained in the cold room for another 45 min (water at 3.8°C). Shivering was determined visually by researchers and/or self-reported by subjects. The shivering threshold was defined as the water temperature at which shivering occurred.<sup>62</sup>

Forty-eight to 72 h after the shivering threshold determination, participants were exposed to a 2-h personalized cooling procedure and BAT parameters were assessed. After resting in a warm room (22°C–24°C), participants were placed in a cool room (19.5°C–20°C) wearing a water-perfused cooling vest (Polar Products Inc., Stow, OH, USA) covering the abdomen, chest, and supraclavicular region. The water temperature was set at 4°C above their shivering threshold. After the first hour of cold exposure, the water temperature was increased by 1°C to avoid shivering (5°C above the individual shivering threshold). If subjects reported shivering, the water temperature was further increased by 1°C.

After 1 h of cold exposure, a bolus of ~185 MBq of <sup>18</sup>F-FDG was intravenously injected. After 2 h of cold exposure, a static PET/CT (Siemens Biograph 16 PET-CT, Erlangen, Germany) scan was performed in the supine position.<sup>25,62–64</sup> PET/CT scans were analyzed using a previously described procedure<sup>62</sup> with the Beth Israel plug-in<sup>63</sup> for FIJI software.<sup>64</sup> An individualized, standardized uptake value (SUV) threshold (i.e., 1.2/[lean body mass/body mass]) and a fixed radiodensity range (–10 to –190 Hounsfield units) were used for BAT quantification.<sup>65–67</sup> The region of interest (ROI) was semi-automatically outlined from the atlas (i.e., cervical vertebra 1) to approximately the mid-chest. BAT volume and <sup>18</sup>F-FDG uptake (i.e., SUVmean SUVpeak) were quantified according to the BARCIST 1.0 recommendations.<sup>65</sup> All scans were visually examined to detect <sup>18</sup>F-FDG uptake in BAT-specific depots. BAT volume was determined as the number of pixels in the above range with an SUV value above the SUV threshold. BAT activity was determined concerning the SUVmean (the mean quantity of <sup>18</sup>F-FDG in the above same pixels) and SUVpeak (the mean of the three highest <sup>18</sup>F-FDG contents in three pixels within a volume of <1 cm<sup>3</sup>). BAT mean radiodensity was determined as the average radiodensity of those voxels meeting the aforementioned criteria in a single ROI covering the body (except the mouth) from the atlas to the thoracic vertebra 4.

The natural calendar day when the baseline and postintervention <sup>18</sup>F-FDG-PET/CT scans were performed was recorded from day 1 (January 1<sup>st</sup>) until day 365/366 (December 31<sup>st</sup>).

### Long-term exercise intervention

An extensive description of the supervised exercise program can be found elsewhere.<sup>59</sup> Following the World Health Organization guidelines, the ACTIBATE supervised exercise intervention combined endurance and resistance training. For 24 weeks, participants attended the research center 3–4 times per week, 60–90 min per session. Participants completed a total of 150 min/week of endurance training (performed in all sessions), executed at 60% of the heart rate reserve (HRres) in the MOD-EX, whereas the VIG-EX performed 75 min/week at 60% HRres and 75 min/week at 80% HRres. The participants completed ~80 min of resistance exercise per week over two sessions with loads equivalent to 50% of the repetition maximum (RM) in the MOD-EX and the 70% RM in the VIG-EX. The load for resistance exercises was individually adjusted monthly.<sup>59</sup>

### Blood sample collection

Before cold exposure, an intravenous catheter was placed in the antecubital vein, and blood was collected before (baseline) and during the cold exposure experiment, at 60 and 120 min. Blood samples for determining cardiometabolic risk factors were collected on a different day between 8 and 11 a.m. after a 10-h fast. Blood was immediately centrifuged to obtain serum (obtained with Vacutainer SST II Advance tubes) and plasma (obtained with Vacutainer Hemogard tubes, containing a salt of ethylenediaminetetraacetic acid as an anticoagulant). Samples were aliquoted and stored at –80°C.

### Determination of plasma signaling lipids

Plasma levels of omega-6 and omega-3 oxylipins, eCBs and analogs, lysophospholipids, and sphingosine-1-phosphate species were determined using a validated liquid chromatography-tandem mass spectrometry (LC-MS/MS) method as described elsewhere.<sup>47</sup> Briefly, plasma samples were prepared by liquid-liquid extraction and analyzed using a Shimadzu LC system (Shimadzu Corporation, Kyoto, Japan) connected to an SCIEX QTRAP 7500<sup>+</sup> mass spectrometer (SCIEX, Framingham, MA, USA). The LC-MS/MS protocol enabled the analysis of oxylipins derived from the omega-6 polyunsaturated fatty acids (PUFAs) [i.e., linoleic acid (LA), dihomo- $\gamma$ -linolenic acid (DGLA), arachidonic acid (AA), and adrenic acid (AdRA)], as well as the oxylipins derived from omega-3 PUFAs [i.e.,  $\alpha$ -linolenic acid (ALA), eicosapentaenoic acid (EPA), and docosahexaenoic acid (DHA)]. We also analyzed eCBs [i.e., anandamide (AEA) and 1-Arachidonoylglycerol and 2-Arachidonoylglycerol (1-AG and 2-AG)] and their analogs [i.e., docosahexaenoylethanolamide (DHEA), 1-linoleoylglycerol and 2-linoleoylglycerol (1-LG and 2-LG) and 1-oleoylglycerol and 2-oleoylglycerol (1-OG and 2-OG)]. The protocol also allowed the determination of cyclic-lysophosphatidic acid (cLPA), lysophosphatidic acid (LPA), lysophosphatidylethanolamine (LPE), lysophosphatidylserine (LPS), lysophosphatidylinositol (LPI), lysophosphatidylglycerol (LPG), platelet-activating factor (PAF), and sphingosine-1-phosphate.

Based on a previously published method which was also described in<sup>26,68</sup> metabolite extraction was performed following a liquid-liquid extraction protocol with minor adaptations by using 50  $\mu$ L plasma. After sample preparation, oxylipins and endocannabinoids were analyzed using a previously validated method.<sup>26,68</sup> Extracted samples were analyzed using a Shimadzu LC system (Shimadzu Corporation, Kyoto, Japan) connected to an SCIEX QTRAP 7500<sup>+</sup> mass spectrometer (AB Sciex, Framingham, MA, USA). Separation was performed using a BEH C18 column (50 mm  $\times$  2.1 mm, 1.7  $\mu$ m) from Waters Technologies (Mildford, MA, USA) maintained at 40°C. The mobile phase was composed of 0.1% acetic acid in water (A), acetonitrile/0.1% acetic acid in methanol (90:10, v/v, B), and 0.1% acetic acid in isopropanol (C). Separations were performed at 40°C at a flow rate of 0.7 mL/min using the following



gradient: 20% B and 1% C as starting conditions, changing to 85% B between 0.75 and 14 min and to 15% C between 11 and 14 min; conditions held for 0.5 min before column re-equilibration at the starting conditions from 14.8 to 16 min.

The ionization of the compounds was performed using electrospray ionization in negative and positive mode with polarity switching. Selected Reaction Mode (SRM) was used for MS/MS acquisition. SRM transitions were individually optimized for targeted analytes and respective internal standards using standard solutions. Isotopically-labeled internal standards are detailed in Table S4.

Lysophospholipids and sphingosine-1-phosphate species were analyzed using a previously validated method.<sup>69</sup> Analyses were performed by a Shimadzu LCMS-8060 system (Shimadzu, Japan) using a Kinetex Core-Shell EVO 100 Å C18 column (50 × 2.1 mm, 1.8 μm; Phenomenex, USA).

For each target compound, the ratio between its peak area and the peak area of its respective internal standard was calculated using SCIEX OS-MQ Software and used for further data analysis. The data quality was monitored using regular injection of quality control (QC) samples, consisting of blank plasma samples, within the sequence. QC samples were used to correct inter-batch variations using the in-house developed mzQuality workflow (available at <http://www.mzQuality.nl>).<sup>70</sup> Relative standard deviations (RSDs) of peak area ratios were calculated for each targeted analyte detected in the QC samples. The RSD obtained for QC samples are listed in Table S3.

### Anthropometric and body composition

Weight and height were measured barefoot and with light clothing, using a Seca scale and stadiometer (model 799; Electronic Column Scale, Seca, Hamburg, Germany), and were used to calculate body mass index (BMI; kg/m<sup>2</sup>). Waist circumference (WC) was measured at the minimum abdominal perimeter at the end of a normal expiration, with the arms relaxed on both sides of the body. When the minimum perimeter could not be detected, measurements were taken just above the umbilicus in a horizontal plane. WC was measured twice with plastic tape; the two obtained measures were averaged for further analyses. Lean mass, fat mass, and visceral adipose tissue (VAT) mass were measured by dual-energy X-ray absorptiometry using a Discovery Wi scanner (Hologic Inc., Bedford, MA, USA). The fat mass percentage was also extracted from this scan.

### Cardiometabolic risk factors

Traditional cardiometabolic risk factors were determined in serum following standard procedures.<sup>7677</sup> Glucose levels were assessed using an AU5832 analyzer (Beckman Coulter, Brea, CA, USA) with a Beckman Coulter reagent (OSR6521). Insulin was measured by chemiluminescence immunoassays using the UniCel Dxl 800 analyzer (Beckman Coulter) with Beckman Coulter chemiluminescent reagents (33410). TC, HDL-C, TG, apolipoproteins A and B, glutamic pyruvic transaminase (GPT), gamma-glutamyl transferase (GGT), and alkaline phosphatase (ALP) were measured using an AU5832 spectrophotometer (Beckman Coulter) with Beckman Coulter reagents (OSR6116, OSR60118, OSR6187, 446410, 447730, OSR6507, OSR6520, and OSR6204). LDL-C (mM) was calculated from the Friedewald formula [ $TC (mM) - HDLc (mM) - 0.45 \times TG (mM)$ ]. C-reactive protein was measured by immunoturbidimetric assays (OSR6299) using an AU5832 spectrophotometer. Leptin and adiponectin were measured in plasma using the MILLIPLEX MAG Human Adipokine Magnetic Bead Panel 2 (Catalog # HADK2MAG-61K) and a MILLIPLEX MAP Human Adipokine Magnetic Bead Panel 1 (Catalog # HADK1MAG-61K), respectively (Luminex Corporation, Austin, TX, USA).

Insulin sensitivity was estimated using the homeostatic model assessment of insulin resistance index (HOMA-IR) calculated as<sup>71</sup>:

$$HOMA - IR = \frac{\text{insulin} \left( \frac{\mu\text{IU}}{\text{mL}} \right) * \text{glucose} \left( \frac{\text{mmol}}{\text{L}} \right)}{22.5}$$

### QUANTIFICATION AND STATISTICAL ANALYSIS

Since the current study was a secondary analysis from the ACTIBATE randomized controlled trial, no specific power calculation was performed.<sup>25</sup> This secondary analysis included all participants with blood sample determinations during the cold exposure sessions. Descriptive data are expressed as mean ± standard deviation unless otherwise stated. Firstly, data normality was explored using the Shapiro-Wilk test, visual histograms, and Q-Q plots. None of the omega-6 and omega-3 oxylipins, eCBs and analogs, lysophospholipids, and sphingosine-1-phosphate species followed a normal distribution. Thereby, all values were log<sub>2</sub> transformed for the analyses. None of the cardiometabolic risk factors followed normal distribution; therefore, their values were log<sub>10</sub> transformed for analyses.

We used repeated measures analysis of variance (ANOVA) to study the effect of 2 h of cold exposure on the plasma signaling lipids in Figures 2, S3, S4, S5, and S6. The log<sub>2</sub> fold changes relative to baseline were calculated for 60 and 120 min. Repeated measures ANOVA analyses were performed using the Statistical Package for the Social Sciences v.26.0 (IBM Corporation, Chicago, IL, USA). Independent samples t-tests were performed to analyze cold-induced differences in plasma signaling lipids (i.e., 120 min fold change) between participants with normal weight and overweight or obesity in Figure S7.

Next, we conducted Pearson partial correlation analyses between cold-induced plasma signaling lipids changes (i.e., 60 and 120min fold changes) and BAT parameters (i.e., BAT volume, SUVmean, SUVpeak, and mean radiodensity) adjusted for the natural calendar day when the baseline <sup>18</sup>F-FDG-PET/CT scan was performed in Figures 3, S8, S9, S10, and S11. Pearson bivariate

correlation analyses were further performed to evaluate the associations between cold-induced plasma signaling lipids changes (i.e., 60 and 120 min fold-changes) and cardiometabolic risk factors in [Figures 4, S12, S13, S14, S15 and S16](#). Additionally, we conducted Pearson bivariate correlation analyses between cold-induced plasma signaling lipids changes and the water temperature of the cooling vest in [Figure S17](#). We also performed Pearson partial correlation analyses between cold-induced plasma signaling lipids changes (i.e., 60 and 120 min fold changes) and cardiometabolic risk factors adjusted for the water temperature of the cooling vest, BAT volume, and BAT SUVpeak in [Figure S18](#). All p values were corrected for multiple comparisons by controlling the false discovery rate (FDR) using the two-stage step-up method of the Benjamini-Hochberg false discovery rate (FDR; 0.25) method.<sup>72</sup> Correlation analyses were performed using the R software version 3.6.0 (R Foundation for Statistical Computing). All analyses were performed for all participants, as well as women, men, normal-weight, and overweight or obese separately.

To investigate whether the 24-week supervised concurrent exercise intervention modified the plasma signaling lipid response to cold exposure, we calculated the change after the intervention in 120 min fold-change (i.e., post-intervention 120 min fold-change *minus* pre-intervention 120 min fold-change, for each lipid). To study the effect of the intervention on each lipid, we performed a one-way ANOVA in [Figure 5](#). Bonferroni post hoc adjustments for multiple comparisons were used to examine group differences. These analyses were performed using the Statistical Package for the Social Sciences v.26.0 (IBM Corporation, Chicago, IL, USA). Figures were built with GraphPad Prism software v.9 (GraphPad Software, San Diego, CA, USA). Statistical significance was set at  $p < 0.05$ .

### ADDITIONAL RESOURCES

This study has been registered on <https://clinicaltrials.gov/>, ID: NCT02365129.

**Cell Reports Medicine, Volume 5**

**Supplemental information**

**Cold-induced changes in plasma signaling lipids are associated with a healthier cardiometabolic profile independently of brown adipose tissue**

**Lucas Jurado-Fasoli, Guillermo Sanchez-Delgado, Xinyu Di, Wei Yang, Isabelle Kohler, Francesc Villarroya, Concepcion M. Aguilera, Thomas Hankemeier, Jonatan R. Ruiz, and Borja Martinez-Tellez**

## Changes in plasma signaling lipids after 2 h of cold exposure are associated with a healthier cardiometabolic profile independently of brown adipose tissue in young adults

Lucas Jurado-Fasoli<sup>1,2</sup>, Guillermo Sanchez-Delgado<sup>1,3,4,5</sup>, Xinyu Di<sup>6</sup>, Wei Yang<sup>6</sup>, Isabelle Kohler<sup>7,8</sup>, Francesc Villarroya<sup>4,9</sup>, Concepcion M Aguilera<sup>4,5,10</sup>, Thomas Hankemeier<sup>6</sup>, Jonatan R. Ruiz<sup>1,4,5,‡,\*</sup>, Borja Martinez-Tellez<sup>1,4,5,11‡,\*</sup>

### Affiliations:

<sup>1</sup>Department of Physical Education and Sports, Faculty of Sports Science, Sport and Health University Research Institute (iMUDS), University of Granada, Carretera de Alfacar s/n, 18071 Granada, Spain-

<sup>2</sup>Department of Physiology, Faculty of Medicine, University of Granada, Granada, Andalucía, Spain.

<sup>3</sup>Division of Endocrinology, Department of Medicine, Centre de Recherche du Centre Hospitalier Universitaire de Sherbrooke, Université de Sherbrooke, Sherbrooke, QC, Canada.

<sup>4</sup>CIBER de Fisiopatología de la Obesidad y Nutrición (CIBEROBN), Instituto de Salud Carlos III, Granada, Spain.

<sup>5</sup>Instituto de Investigación Biosanitaria, Ibs.Granada, Granada, Spain.

<sup>6</sup>Metabolomics and Analytics Center, Leiden Academic Centre for Drug Research (LACDR), Leiden University, Leiden, the Netherlands.

<sup>7</sup>Vrije Universiteit Amsterdam, Amsterdam Institute of Molecular and Life Sciences (AIMMS), Division of BioAnalytical Chemistry, Amsterdam, the Netherlands.

<sup>8</sup>Center for Analytical Sciences Amsterdam, Amsterdam, the Netherlands.

<sup>9</sup>Department of Biochemistry and Molecular Biomedicine, Institute of Biomedicine, Barcelona, Spain.

<sup>10</sup>Department of Biochemistry and Molecular Biology II, "José Mataix Verdú" Institute of Nutrition and Food Technology (INYTA), Biomedical Research Centre (CIBM), University of Granada, Granada, 18016, Spain.

<sup>11</sup>Department of Education, Faculty of Education Sciences and SPORT Research Group (CTS-1024), CERNEP Research Center, University of Almería, Almería, Spain.

‡Lead author

‡These authors contributed equally

\*Corresponding authors: [ruizj@ugr.es](mailto:ruizj@ugr.es) & [borjammt@gmail.com](mailto:borjammt@gmail.com).

## SUPPLEMENTARY MATERIAL

**Table S1.** STROBE Statement—checklist of items that should be included in reports of observational studies. Related to Table 1 and Figures 1-4.

	Item No.	Recommendation	Page No.
<b>Title and abstract</b>	1	(a) Indicate the study's design with a commonly used term in the title or the abstract	2
		(b) Provide in the abstract an informative and balanced summary of what was done and what was found	2
<b>Introduction</b>			
Background/rationale	2	Explain the scientific background and rationale for the investigation being reported	3,4
Objectives	3	State specific objectives, including any prespecified hypotheses	5
<b>Methods</b>			
Study design	4	Present key elements of study design early in the paper	22-23
Setting	5	Describe the setting, locations, and relevant dates, including periods of recruitment, exposure, follow-up, and data collection	22
Participants	6	(a) <i>Cohort study</i> —Give the eligibility criteria, and the sources and methods of selection of participants. Describe methods of follow-up	21,22
		<i>Case-control study</i> —Give the eligibility criteria, and the sources and methods of case ascertainment and control selection. Give the rationale for the choice of cases and controls	
		<i>Cross-sectional study</i> —Give the eligibility criteria, and the sources and methods of selection of participants	
		(b) <i>Cohort study</i> —For matched studies, give matching criteria and number of exposed and unexposed	N/A
		<i>Case-control study</i> —For matched studies, give matching criteria and the number of controls per case	
Variables	7	Clearly define all outcomes, exposures, predictors, potential confounders, and effect modifiers. Give diagnostic criteria, if applicable	23
Data sources/measurement	8*	For each variable of interest, give sources of data and details of methods of assessment (measurement). Describe comparability of assessment methods if there is more than one group	23-26
Bias	9	Describe any efforts to address potential sources of bias	23-26
Study size	10	Explain how the study size was arrived at	26
Quantitative variables	11	Explain how quantitative variables were handled in the analyses. If applicable, describe which groupings were chosen and why	26
Statistical methods	12	(a) Describe all statistical methods, including those used to control for confounding	26-28
		(b) Describe any methods used to examine subgroups and interactions	26-28
		(c) Explain how missing data were addressed	26-28
		(d) <i>Cohort study</i> —If applicable, explain how loss to follow-up was addressed	N/A
		<i>Case-control study</i> —If applicable, explain how matching of cases and controls was addressed	

		<i>Cross-sectional study</i> —If applicable, describe analytical methods taking account of sampling strategy	
		(e) Describe any sensitivity analyses	26-28
<b>Results</b>			
Participants	13*	(a) Report numbers of individuals at each stage of study—eg numbers potentially eligible, examined for eligibility, confirmed eligible, included in the study, completing follow-up, and analysed	Figure S1
		(b) Give reasons for non-participation at each stage	Figure S1
		(c) Consider use of a flow diagram	Figure S1
Descriptive data	14*	(a) Give characteristics of study participants (eg demographic, clinical, social) and information on exposures and potential confounders	Table 1
		(b) Indicate number of participants with missing data for each variable of interest	Table 1
		(c) <i>Cohort study</i> —Summarise follow-up time (eg, average and total amount)	N/A
Outcome data	15*	<i>Cohort study</i> —Report numbers of outcome events or summary measures over time	
		<i>Case-control study</i> —Report numbers in each exposure category, or summary measures of exposure	
		<i>Cross-sectional study</i> —Report numbers of outcome events or summary measures	6
Main results	16	(a) Give unadjusted estimates and, if applicable, confounder-adjusted estimates and their precision (eg, 95% confidence interval). Make clear which confounders were adjusted for and why they were included	
		(b) Report category boundaries when continuous variables were categorized	
		(c) If relevant, consider translating estimates of relative risk into absolute risk for a meaningful time period	
Other analyses	17	Report other analyses done—eg analyses of subgroups and interactions, and sensitivity analyses	6-9
<b>Discussion</b>			
Key results	18	Summarise key results with reference to study objectives	10
Limitations	19	Discuss limitations of the study, taking into account sources of potential bias or imprecision. Discuss both direction and magnitude of any potential bias	15
Interpretation	20	Give a cautious overall interpretation of results considering objectives, limitations, multiplicity of analyses, results from similar studies, and other relevant evidence	10-14
Generalisability	21	Discuss the generalisability (external validity) of the study results	10-15
<b>Other information</b>			
Funding	22	Give the source of funding and the role of the funders for the present study and, if applicable, for the original study on which the present article is based	16

\*Give information separately for cases and controls in case-control studies and, if applicable, for exposed and unexposed groups in cohort and cross-sectional studies.

**Table S2.** 2017 CONSORT checklist of information to include when reporting a randomized trial assessing nonpharmacologic treatments (NPTs). Related to Figure 5.

Section/Topic Item	Checklist item no.	CONSORT item	Extension for NPT trials	Reported on page n°
<b>Title and abstract</b>				
	1a	Identification as a randomized trial in the title		N/A
	1b	Structured summary of trial design, methods, results, and conclusions (for specific guidance see CONSORT for abstracts)	<i>Refer to CONSORT extension for abstracts for NPT trials</i>	N/A
<b>Introduction</b>				
Background and objectives	2a	Scientific background and explanation of rationale		3-4
	2b	Specific objectives or hypotheses		5
<b>Methods</b>				
Trial design	3a	Description of trial design (such as parallel, factorial) including allocation ratio	When applicable, how care providers were allocated to each trial group	22
	3b	Important changes to methods after trial commencement (such as eligibility criteria), with reasons		22
Participants	4a	Eligibility criteria for participants	When applicable, eligibility criteria for centers and for <i>care providers</i>	21
	4b	Settings and locations where the data were collected		22
Interventions <sup>†</sup>	5	The interventions for each group with sufficient details to allow replication, including how and when they were actually administered	Precise details of both the experimental treatment and comparator	22-23
	5a		Description of the different components of the interventions and, when applicable, description of the procedure for tailoring the interventions to individual participants.	22-23
	5b		Details of <i>whether and how</i> the interventions were standardized.	22-23
	5c		Details of <i>whether and how</i> adherence of care providers to the protocol was assessed or enhanced	22-23
	5d		<i>Details of whether and how adherence of participants to interventions was assessed or enhanced</i>	22-23
Outcomes	6a	Completely defined pre-specified primary and secondary outcome measures, including how and when they were assessed		23-26
	6b	Any changes to trial outcomes after the trial commenced, with reasons		23
Sample size	7a	How sample size was determined	When applicable, details of whether and how the clustering by care providers or centers was addressed	26

Section/Topic Item	Checklist item no.	CONSORT item	Extension for NPT trials	Reported on page n°
	7b	When applicable, explanation of any interim analyses and stopping guidelines		N/A
<b>Randomization:</b>				
- Sequence generation	8a	Method used to generate the random allocation sequence		22-23
	8b	Type of randomization; details of any restriction (such as blocking and block size)		22-23
- Allocation concealment mechanism	9	Mechanism used to implement the random allocation sequence (such as sequentially numbered containers), describing any steps taken to conceal the sequence until interventions were assigned		22-23
- Implementation	10	Who generated the random allocation sequence, who enrolled participants, and who assigned participants to interventions		22-23
Blinding	11a	If done, who was blinded after assignment to interventions (for example, participants, care providers, those assessing outcomes) and how	<del>Whether or not those administering co-interventions were blinded to group assignment</del> If done, who was blinded after assignment to interventions (e.g., participants, care providers, <i>those administering co-interventions</i> , those assessing outcomes) and how	22-23
	11b	If relevant, description of the similarity of interventions	<del>If blinded, method of blinding and description of the similarity of interventions</del>	Not relevant
	11c		<i>If blinding was not possible, description of any attempts to limit bias</i>	22-23
Statistical methods	12a	Statistical methods used to compare groups for primary and secondary outcomes	When applicable, details of whether and how the clustering by care providers or centers was addressed	26-28
	12b	Methods for additional analyses, such as subgroup analyses and adjusted analyses		26-28
<b>Results</b>				
Participant flow (a diagram is strongly recommended)	13a	For each group, the numbers of participants who were randomly assigned, received intended treatment, and were analyzed for the primary outcome	The number of care providers or centers performing the intervention in each group and the number of patients treated by each care provider or in each center	Figure S1
	13b	For each group, losses and exclusions after randomization, together with reasons		Figure S1
	13c		<i>For each group, the delay between randomization and the initiation of the intervention</i>	N/A
	new		Details of the experimental treatment and comparator as they were implemented	N/A
Recruitment	14a	Dates defining the periods of recruitment and follow-up		



Section/Topic Item	Checklist item no.	CONSORT item	Extension for NPT trials	Reported on page n°
	14b	Why the trial ended or was stopped		
Baseline data	15	A table showing baseline demographic and clinical characteristics for each group	When applicable, a description of care providers (case volume, qualification, expertise, etc.) and centers (volume) in each group.	Table 1 and S5
Numbers analyzed	16	For each group, number of participants (denominator) included in each analysis and whether the analysis was by original assigned groups		Figure S1
Outcomes and estimation	17a	For each primary and secondary outcome, results for each group, and the estimated effect size and its precision (such as 95% confidence interval)		6-9
	17b	For binary outcomes, presentation of both absolute and relative effect sizes is recommended		Not binary outcomes
Ancillary analyses	18	Results of any other analyses performed, including subgroup analyses and adjusted analyses, distinguishing pre-specified from exploratory		6-9
Harms	19	All important harms or unintended effects in each group (for specific guidance see CONSORT for harms)		None
<b>Discussion</b>				
Limitations	20	Trial limitations, addressing sources of potential bias, imprecision, and, if relevant, multiplicity of analyses	In addition, take into account the choice of the comparator, lack of or partial blinding, and unequal expertise of care providers or centers in each group	15
Generalizability	21	Generalizability (external validity, applicability) of the trial findings	Generalizability (external validity) of the trial findings according to the intervention, comparators, patients, and care providers and centers involved in the trial	10-15
Interpretation	22	Interpretation consistent with results, balancing benefits and harms, and considering other relevant evidence		10-15
<b>Other information</b>				
Registration	23	Registration number and name of trial registry		21
Protocol	24	Where the full trial protocol can be accessed, if available		Reference 53
Funding	25	Sources of funding and other support (such as supply of drugs), role of funders		16

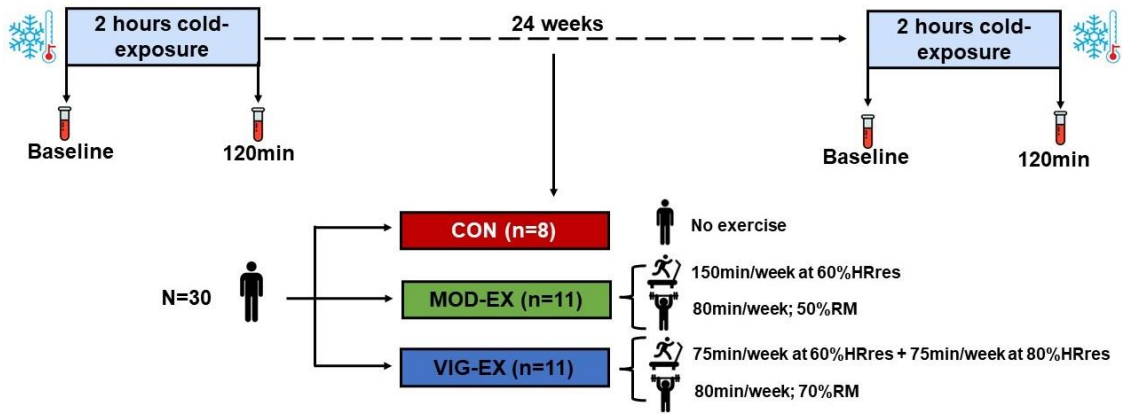
**Table S4.** List of internal standards used in the LC-MS/MS method, related to STAR Methods.

<b>Abbreviation</b>	<b>Name (International Union of Pure and Applied Chemistry, IUPAC)</b>
Arachidonic acid-d <sub>8</sub> C20:4-w6-d <sub>8</sub>	5Z,8Z,11Z,14Z-eicosatetraenoic acid-d8
Docosahexaenoic acid-d <sub>5</sub> (C22:6-w3-d <sub>5</sub> )	4Z,7Z,10Z,13Z,16Z,19Z-docosahexaenoic acid-d5
Linoleic acid-d <sub>4</sub> (C18:2-w6-d <sub>4</sub> )	9Z,12Z-octadecadienoic acid-d4
d <sub>11</sub> -5-iPF <sub>2a</sub> -VI	(8β)-5,9α,11α-trihydroxy-prosta-6E,14Z-dien-1-oic acid-d11
d <sub>4</sub> -8-iso-PGE <sub>2</sub>	9-oxo-11α,15S-dihydroxy-(8β)-prosta-5Z,13E-dien-1-oic acid-d4
d <sub>4</sub> -8-iso-PGF <sub>2α</sub>	9α,11α,15S-trihydroxy-(8β)-prosta-5Z,13E-dien-1-oic acid-d4
d <sub>4</sub> -PGD <sub>2</sub>	9α,15S-dihydroxy-11-oxo-prosta-5Z,13E-dien-1-oic acid-d4
d <sub>4</sub> -PGF <sub>2α</sub>	9S,11R,15S-trihydroxy-5Z,13E-prostadienoic acid-d4
d <sub>9</sub> -PGE <sub>2</sub>	9-oxo-11R,15S-dihydroxy-5Z,13E-prostadienoic acid-d9
d <sub>4</sub> -iPF <sub>2a</sub> -IV	(8S)-10-[(1R,2S,3S,5R)-3,5-Dihydroxy-2-pentylcyclopentyl]-8-hydroxydeca-5,9-dienoic acid-d4
d <sub>11</sub> -8,12-iso-iPF <sub>2a</sub> -VI	(12α)-5,9α,11α-trihydroxy-prosta-6E,14Z-dien-1-oic acid-d11
d <sub>17</sub> -10-Nitrooleate	10-nitro,9Z,12Z-octadecadienoic acid-d17
d <sub>11</sub> -14,15-DiHETrE	14,15-dihydroxy-5Z,8Z,11Z-eicosatrienoic acid-d11
d <sub>4</sub> -9(S)-HODE	9S-hydroxy-10E,12Z-octadecadienoic acid-d4
d <sub>4</sub> -LTB <sub>4</sub>	5S,12R-dihydroxy-6Z,8E,10E,14Z-eicosatetraene-1,20-dioic acid-d4
d <sub>4</sub> -TXB <sub>2</sub>	9S,11,15S-trihydroxy-thromboxa-5Z,13E-dien-1-oic acid-d4
d <sub>6</sub> -20-HETE	20-hydroxy-5Z,8Z,11Z,14Z-eicosatetraenoic acid-d6
d <sub>8</sub> -12(S)-HETE	12S-hydroxy-5Z,8Z,10E,14Z-eicosatetraenoic acid-d8
d <sub>8</sub> -5(S)-HETE	5S-hydroxy-6E,8Z,11Z,14Z-eicosatetraenoic acid-d8
d <sub>4</sub> -(+/-)12,13-DiHOME	12,13-dihydroxy-9Z-octadecenoic acid -d4
d <sub>8</sub> -2-AG	2-(5Z,8Z,11Z,14Z-eicosatetraenoyl)-sn-glycerol-d8
d <sub>8</sub> -AEA	N-(5Z,8Z,11Z,14Z-eicosatetraenoyl)-ethanolamine-d8
d <sub>4</sub> -COR	11β,17,21-trihydroxypregn-4-ene-3,20-dione-d4
d <sub>4</sub> -DHEA	N-(4Z,7Z,10Z,13Z,16Z,19Z-docosahexaenoyl)-ethanolamine-d4
d <sub>4</sub> -LEA	N-(9Z,12Z-octadecadienoyl)-ethanolamine-d4
d <sub>4</sub> -OEA	N-(9Z-octadecenoyl)-ethanolamine-d4
d <sub>4</sub> -PEA	N-hexadecanoyl-ethanolamine-d4
d <sub>3</sub> -SEA	N-(Octadecanoyl)-ethanolamine-d3
LPA C17:0	1-heptadecanoyl-2-hydroxy-sn-glycero-3-phosphate
S-1-P C17:1	2S-amino-4E-heptadecene-1,3R-diol, 1- (dihydrogen phosphate)
cLPA C17:0	1-heptadecanoyl-glycero-2,3-cyclic-phosphate
Spha-1-P C17:0	D-erythro-sphinganine-1-phosphate
Spha C17:0	2S-amino-1,3R-heptadecanediol
Spha C17:1	2S-amino-4E-heptadecene-1,3R-diol
PAF C16:0-d <sub>4</sub>	1-O-hexadecyl-(7,7,8,8-d <sub>4</sub> )-2-O-acetyl-sn-glyceryl-3-phosphorylcholine
LPI C17:1	1-(10Z-heptadecenoyl)-2-hydroxy-sn-glycero-3-phospho-(1'-myo-inositol)
LPS C17:1	1-(10Z-heptadecenoyl)-2-hydroxy-sn-glycero-3-[phospho-L-serine]
LPG C17:1	1-(10Z-heptadecenoyl)-sn-glycero-3-phospho-(1'-rac-glycerol)
LPE C17:1	1-(10Z-heptadecenoyl)-sn-glycero-3-phosphoethanolamine

**Table S5.** Baseline characteristics of the study participants completing the exercise intervention (N=30). Related to Table 1 and Figure 5.

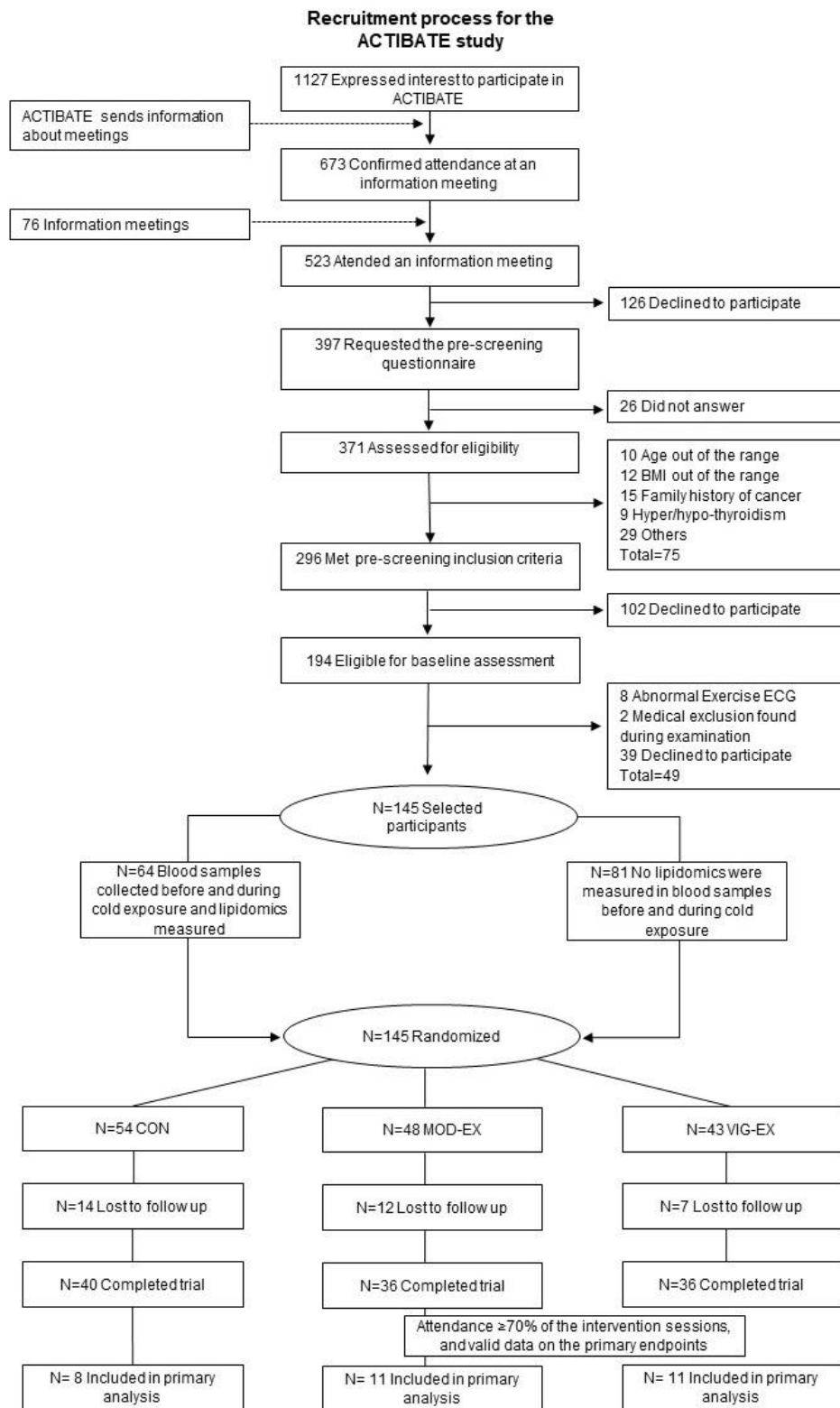
	<b>Control (n=8)</b>		<b>MOD-EX (n=11)</b>		<b>VIG-EX (n=11)</b>	
	Mean	SD	Mean	SD	Mean	SD
Age (years)	21.6	2.5	21.5	2.2	21.6	2.5
<i>Body composition</i>						
BMI (kg/m <sup>2</sup> )	21.9	2.0	24.9	4.4	25.3	4.9
Waist circumference (cm)	74.3	9.5	81.1	12.2	82.9	14.3
Lean mass (kg)	40.8	8.0	41.5	9.4	40.6	9.5
Fat mass (kg)	18.7	5.2	24.7	8.7	26.7	7.2
Fat mass (%)	30.4	7.2	35.7	8.3	38.3	4.0
VAT mass (g)	242.3	107.6	332.5	170.3	352.2	191.4
<i>Cardiometabolic risk factors</i>						
Glucose (mg/dL)	87.3	6.1	86.6	7.7	86.9	6.5
Insulin (μIU/mL)	6.0	3.2	8.2	2.6	7.7	4.5
HOMA-IR	1.3	0.8	1.8	0.7	1.7	1.2
Insulin glucose ratio	10.2	4.8	14.4	3.9	13.3	6.3
Total cholesterol (mg/dL)	149.6	12.1	161.5	28.0	182.8	36.7
HDL-C (mg/dL)	55.0	7.7	56.9	15.5	56.6	15.9
LDL-C (mg/dL)	82.9	13.8	89.5	19.2	102.7	24.2
Tryglicerides (mg/dL)	58.5	26.1	75.3	31.5	117.7	58.9
APOA1 (mg/dL)	149.3	13.8	168.4	57.3	164.5	37.4
APOB (mg/dL)	56.7	8.6	63.9	16.7	77.6	22.5
Leptin (μg/L)	2.9	1.2	6.2	5.2	7.3	3.7
Adiponectin (mg/L)	10.8	5.3	10.0	4.3	10.3	6.7
GTP (IU/L)	15.5	6.3	14.1	4.3	21.9	12.3
GGT (IU/L)	16.4	9.2	14.1	4.4	19.36	12.3
ALP (IU/L)	73.4	32.3	80.8	23.8	79.5	20.2
C-reactive protein (mg/L)	1.1	0.9	3.2	3.8	1.6	1.1
<i>Brown adipose tissue</i>						
BAT volume (mL)	60.8	58.4	83.4	70.0	62.8	62.1
BAT SUV <sub>mean</sub>	3.6	1.1	4.1	1.9	3.8	1.7
BAT SUV <sub>peak</sub>	10.8	6.7	11.6	9.0	11.3	8.2
BAT radiodensity (HU)	-59.5	6.4	-58.8	7.4	-59.3	9.0

Data presented as mean and standard deviation (SD). *Abbreviations:* ALP, alkaline phosphatase; APOA1, apolipoprotein A1; APOB, apolipoprotein B; BAT, brown adipose tissue; BMI, body mass index; CON, control group; GGT, gamma-glutamyl transferase; GTP, glutamic pyruvic transaminase; HDL-C, high-density lipoprotein cholesterol; HOMA-IR, homeostatic model assessment of insulin resistance index; HU, Hounsfield units; LDL-C, low-density lipoprotein cholesterol; MOD-EX, moderate-intensity exercise group; SUV, standardized uptake value; VAT, visceral adipose tissue; VIG-EX, vigorous-intensity exercise group.



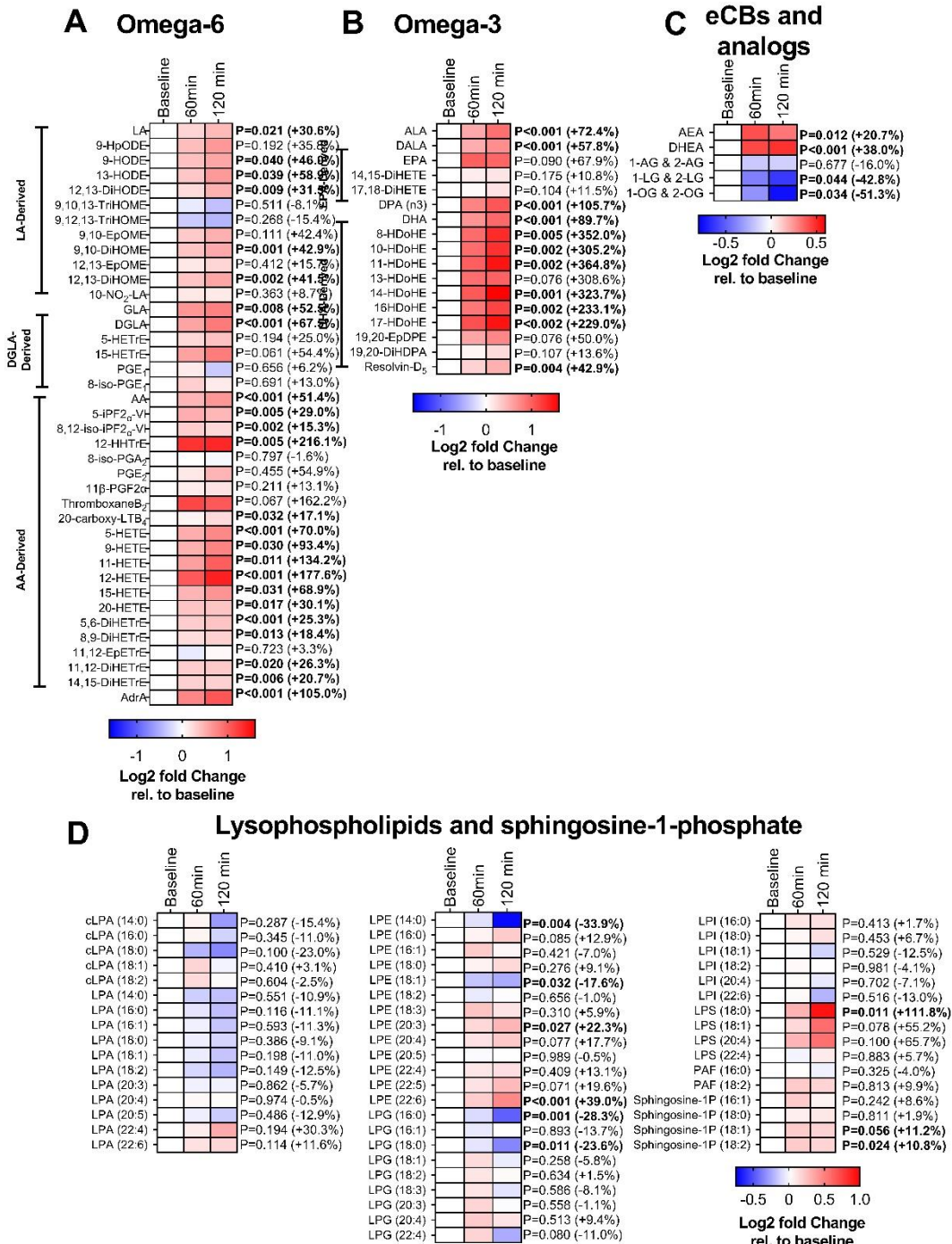
**Figure S1. Design of the study investigating the influence of a 24-week supervised concurrent exercise intervention on plasma lipidome response to cold exposure in young adults. Related to Figure 1 and 5.**

*Abbreviations:* CON, control group; HRres, heart rate reserve; min: minutes; MOD-EX, moderate-intensity exercise group; RM, repetition maximum; VIG-EX, vigorous-intensity exercise group.



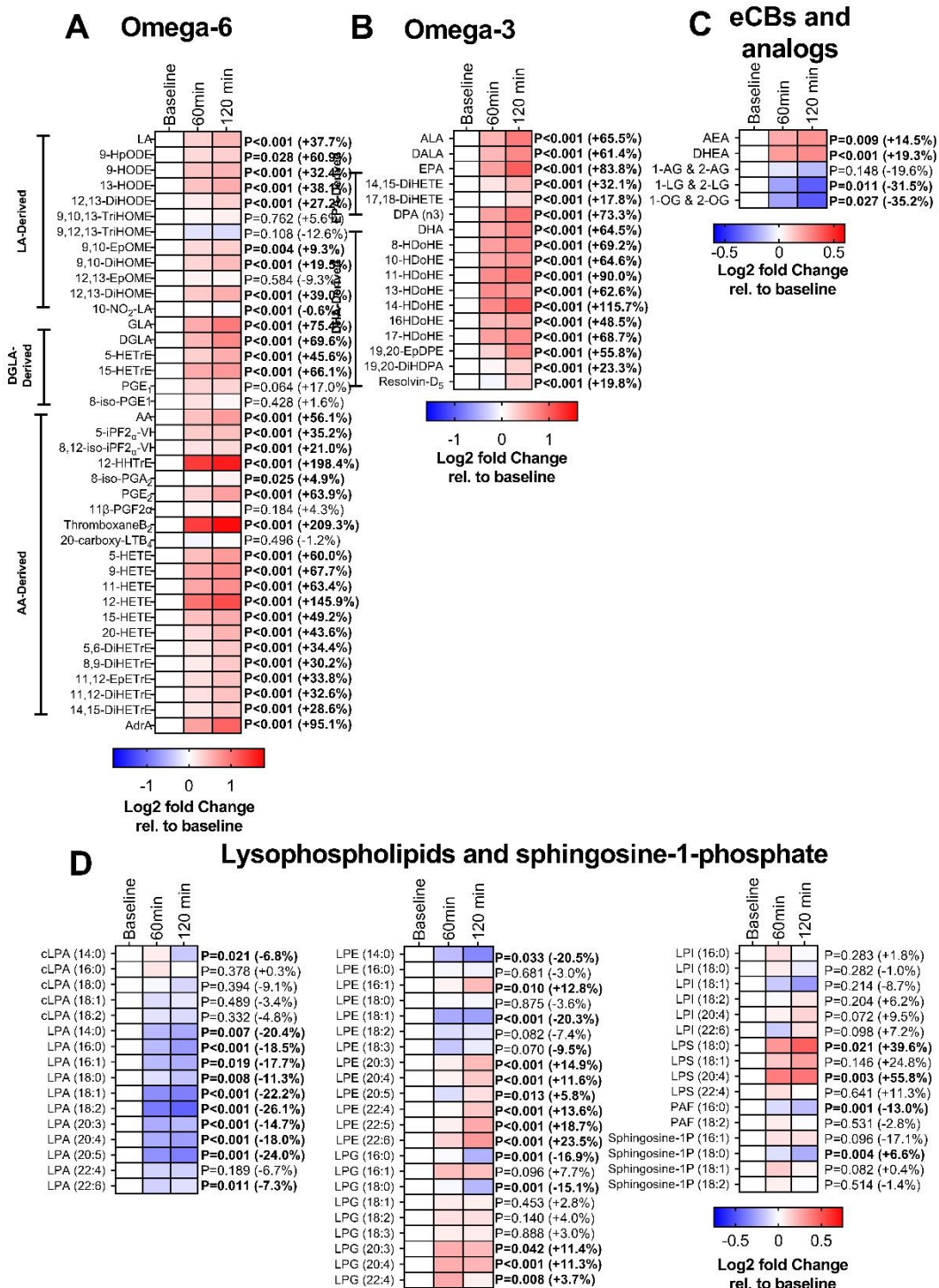
**Figure S2. Study participants enrolment from the ACTIBATE study. Related to Figure 1.**

*Abbreviations:* BMI, body mass index; CON, control group; MOD-EX, moderate-intensity exercise group; VIG-EX: vigorous-intensity exercise group; ECG, electrocardiogram.



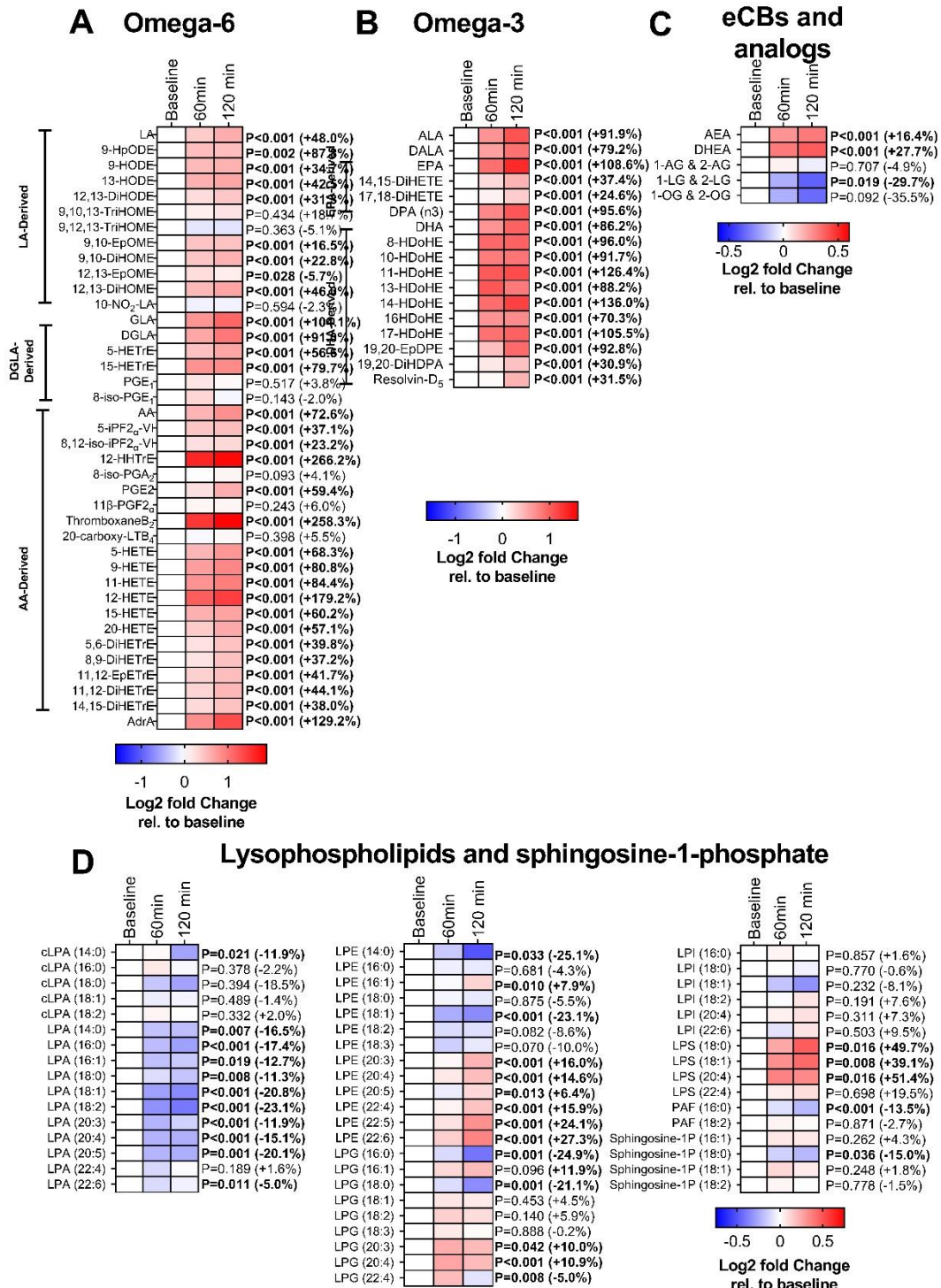
**Figure S3. Effects of 2 h of cold exposure on the plasma levels of omega-6 oxylipins (A), omega-3 oxylipins (B), endocannabinoids and analogs (eCBs, C), and lysophospholipids and sphingosine-1-phosphate (D) in men (n=17). Related to Figure 2.**

The color of the squares represents the mean log2 fold change of the area peak ratio of that timepoint relative to baseline. Red color represents an increase, whereas blue represents a decrease. P-values obtained from repeated measures analyses of variance (ANOVA). Values in brackets represent the mean percentage of change at 120 min relative to the baseline of each lipid. The name and abbreviations of signaling lipids are detailed in Table S3.



**Figure S4. Effects of 2 h of cold exposure on the plasma levels of omega-6 oxylinpns (A), omega-3 oxylinpns (B), endocannabinoids and analogs (eCBs, C), and lysophospholipids and sphingosine-1-phosphate (D) in women (n=47). Related to Figure 2.**

The color of the squares represents the mean log2 fold change of the area peak ratio of that timepoint relative to baseline. Red color represents an increase, whereas blue represents a decrease. P-values obtained from repeated measures analyses of variance (ANOVA). Values in brackets represent the mean percentage of change at 120 min relative to the baseline of each lipid. The name and abbreviations of signaling lipids are detailed in Table S3.





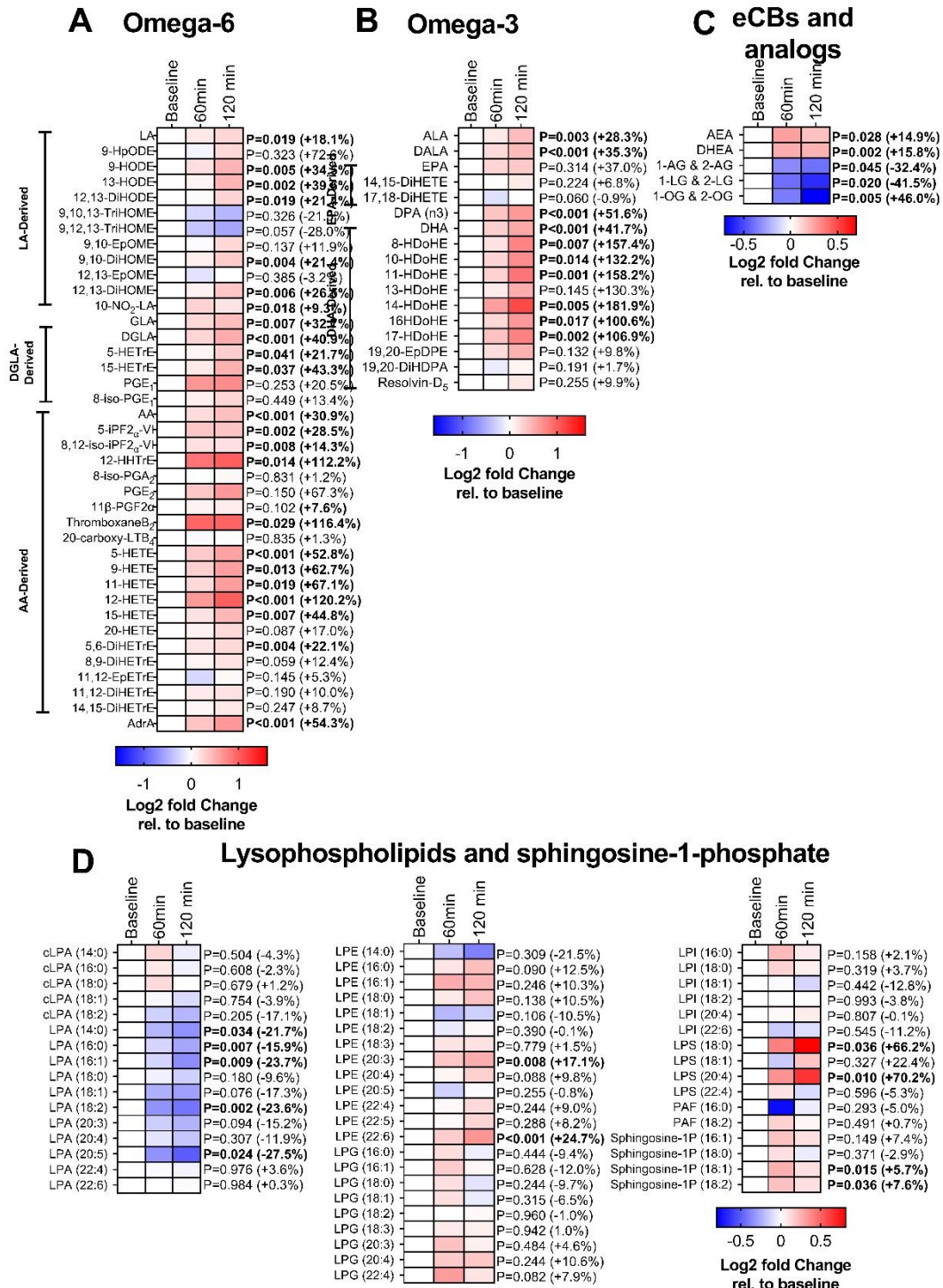


**Figure S6. Effects of 2 h of cold exposure on the plasma levels of omega-6 oxylipins (A), omega-3 oxylipins (B), endocannabinoids and analogs (eCBs, C), and lysophospholipids and sphingosine-1-phosphate (D) in participants with overweight or obesity (n=21). Related to Figure 2.**

The color of the squares represents the mean log<sub>2</sub> fold change of the area peak ratio of that timepoint relative to baseline. Red color represents an increase, whereas blue represents a decrease. P-values obtained from repeated measures analyses of variance (ANOVA). Values in brackets represent the mean percentage of change at 120 min relative to the baseline of each lipid. The name and abbreviations of signaling lipids are detailed in Table S3.

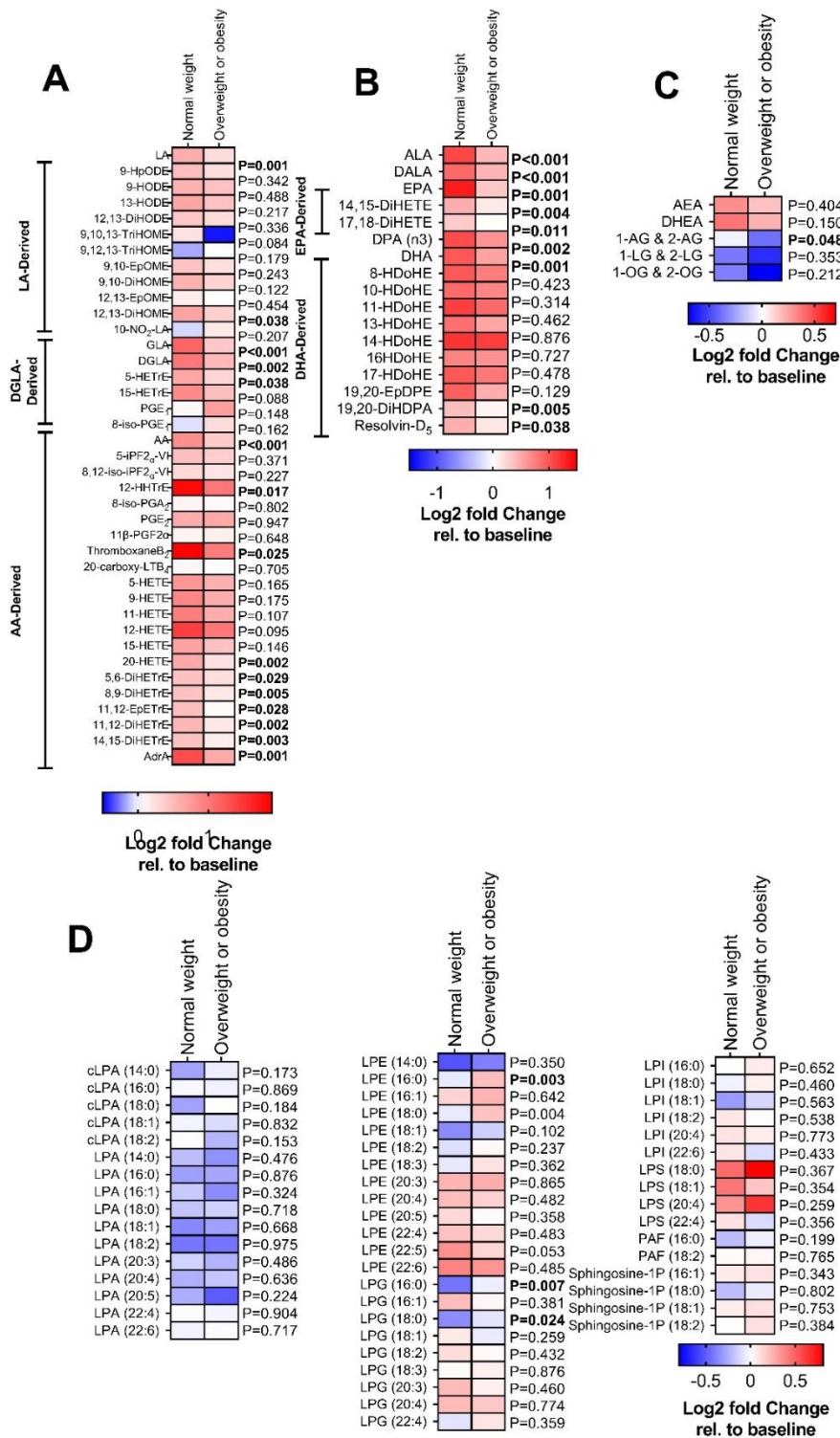


**Figure S7. Differences in cold-induced changes in the plasma levels of omega-6 oxylipins (A), omega-3 oxylipins (B), endocannabinoids and analogs (eCBs, C), and lysophospholipids and sphingosine-1-phosphate sphingolipids (D) between participants with normal weight and participants with overweight or obesity. Related to Figure 2.**

The color of the squares represents the mean log<sub>2</sub> fold change of the area peak ratio of the 120 min relative to baseline. Red color represents an increase, whereas blue represents a decrease. P-values obtained from independent samples t-test.

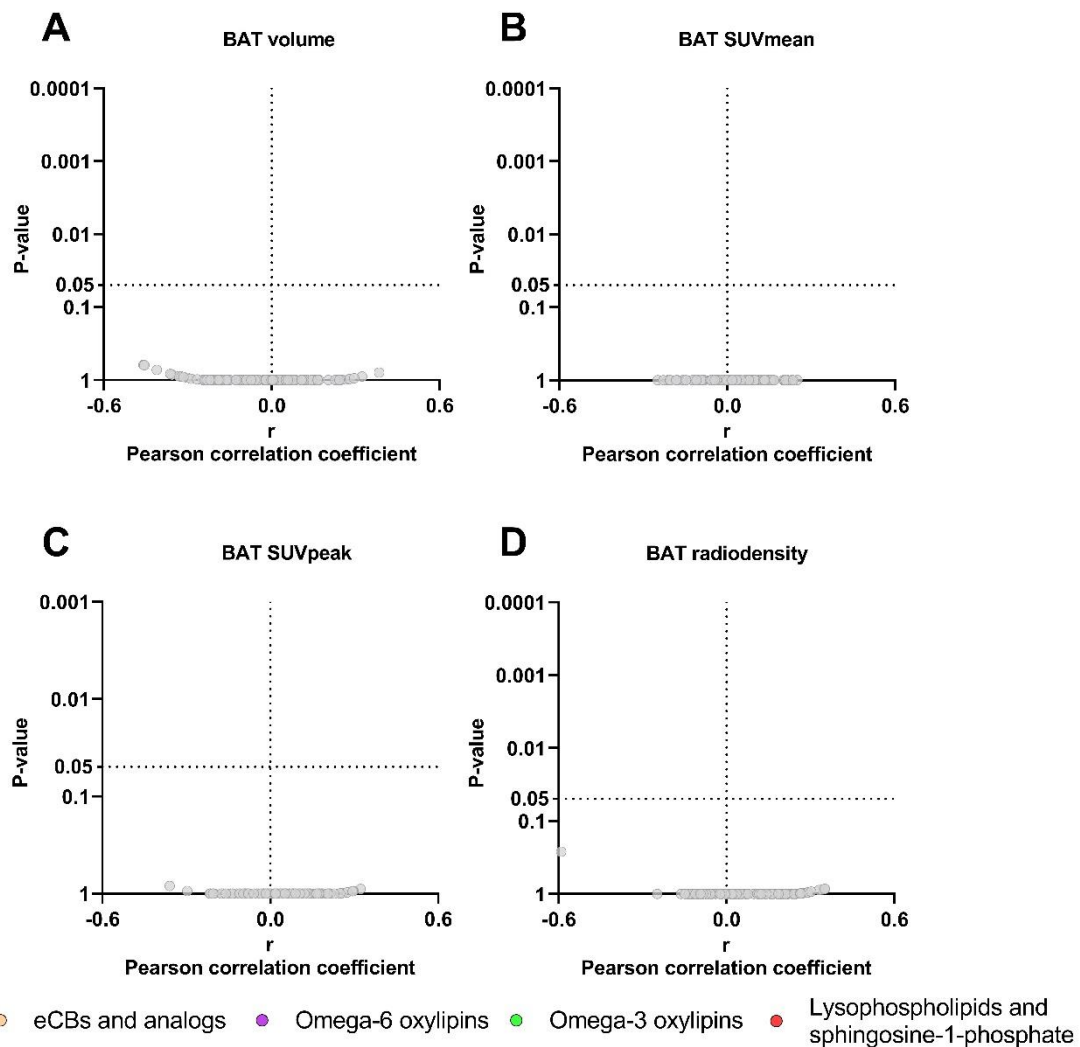


**Figure S8. Association between cold-induced changes in the plasma levels of signaling lipids and brown adipose tissue-related outcomes in men (n=17). Related to Figure 3.**

Volcano plots showing partial correlation analyses between the 120 min fold-change relative to baseline and BAT volume (A), BAT SUVmean (B), BAT SUVpeak (C), and BAT radiodensity (D, n=13). Partial correlation analyses were adjusted for the natural calendar day when the baseline  $^{18}\text{F}$ -FDG-PET/CT scan was performed. The X-axis represents Pearson partial correlation coefficients, whereas the Y-axis represents the FDR-adjusted P-values of the correlations. Grey dots represent non-significant correlations, whereas colored dots represent statistically significant correlations (P-value<0.05 after FDR correction). *Abbreviations:* BAT, brown adipose tissue; eCBs, endocannabinoids; SUV, standardized uptake value.

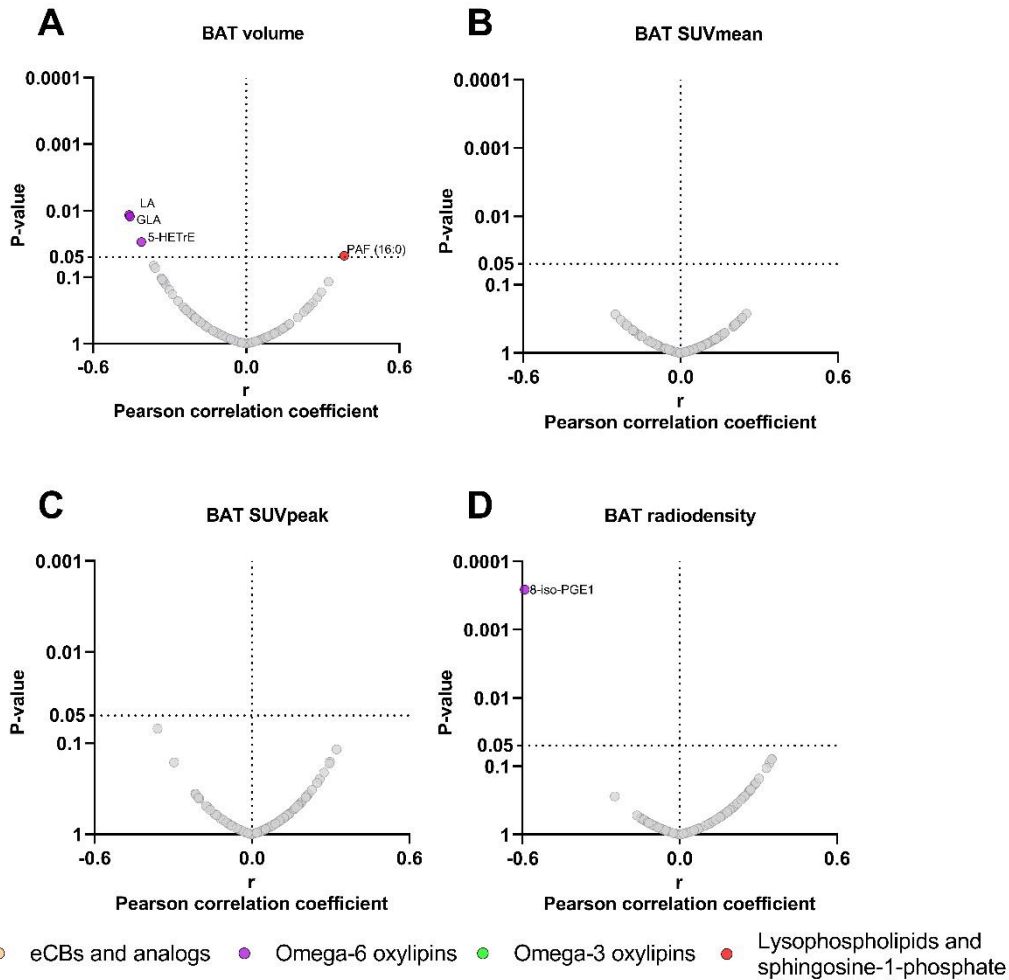


**Figure S9. Association between cold-induced changes in the plasma levels of signaling lipids and brown adipose tissue-related outcomes in women (n=47). Related to Figure 3.**

Volcano plots showing partial correlation analyses between the 120 min fold-change relative to baseline and BAT volume (A), BAT SUVmean (B), BAT SUVpeak (C), and BAT radiodensity (D, n=34). Partial correlation analyses were adjusted for the natural calendar day when the baseline  $^{18}\text{F}$ -FDG-PET/CT scan was performed. The X-axis represents Pearson partial correlation coefficients, whereas the Y-axis represents the FDR-adjusted P-values of the correlations. Grey dots represent non-significant correlations, whereas colored dots represent statistically significant correlations (P-value<0.05 after FDR correction). *Abbreviations:* BAT, brown adipose tissue; eCBs, endocannabinoids; SUV, standardized uptake value.

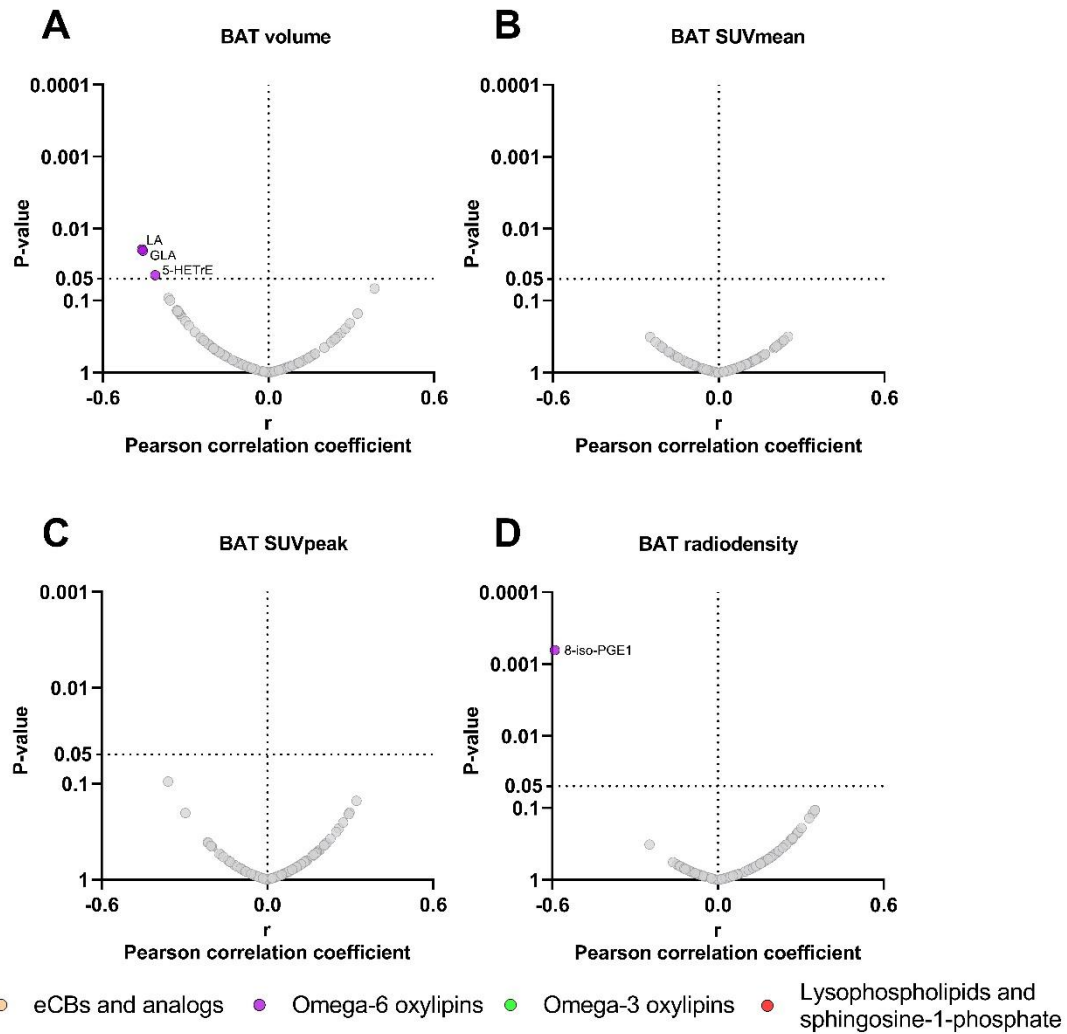


**Figure S10. Association between cold-induced changes in the plasma levels of signaling lipids and brown adipose tissue-related outcomes in participants with normal-weight (n=47). Related to Figure 3.**

Volcano plots showing partial correlation analyses between the 120 min fold-change relative to baseline and BAT volume (A), BAT SUVmean (B), BAT SUVpeak (C), and BAT radiodensity (D, n=33). Partial correlation analyses were adjusted for the natural calendar day when the baseline  $^{18}\text{F}$ -FDG-PET/CT scan was performed. The X-axis represents Pearson partial correlation coefficients, whereas the Y-axis represents the FDR-adjusted P-values of the correlations. Grey dots represent non-significant correlations, whereas colored dots represent statistically significant correlations (P-value<0.05 after FDR correction). *Abbreviations:* BAT, brown adipose tissue; eCBs, endocannabinoids; SUV, standardized uptake value.

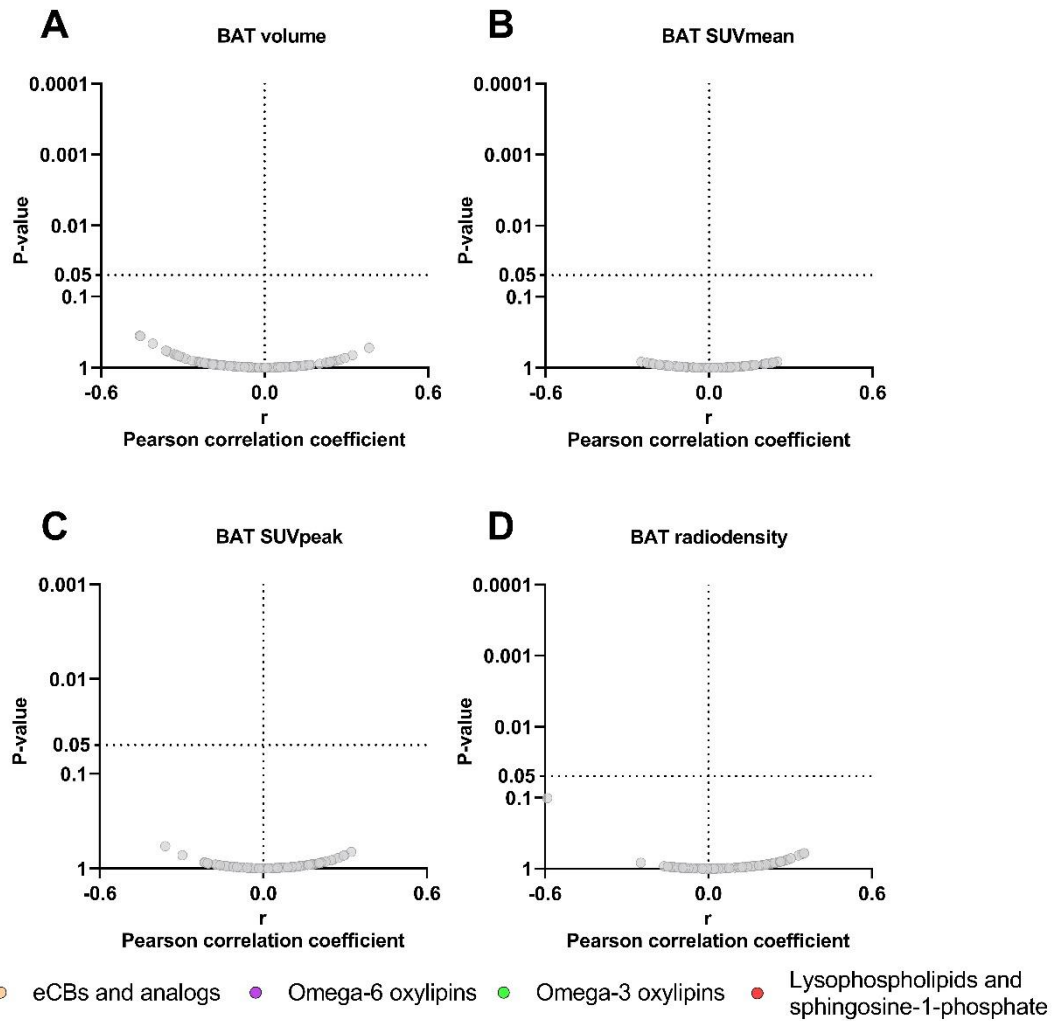


**Figure S11. Association between cold-induced changes in the plasma levels of signaling lipids and brown adipose tissue-related outcomes in participants with overweight or obesity (n=21). Related to Figure 3.**

Volcano plots showing partial correlation analyses between the 120 min fold-change relative to baseline and BAT volume (A), BAT SUVmean (B), BAT SUVpeak (C), and BAT radiodensity (D, n=14). Partial correlation analyses were adjusted for the natural calendar day when the baseline  $^{18}\text{F}$ -FDG-PET/CT scan was performed. The X-axis represents Pearson partial correlation coefficients, whereas the Y-axis represents the FDR-adjusted P-values of the correlations. Grey dots represent non-significant correlations, whereas colored dots represent statistically significant correlations (P-value<0.05 after FDR correction). *Abbreviations:* BAT, brown adipose tissue; eCBs, endocannabinoids; SUV, standardized uptake value.

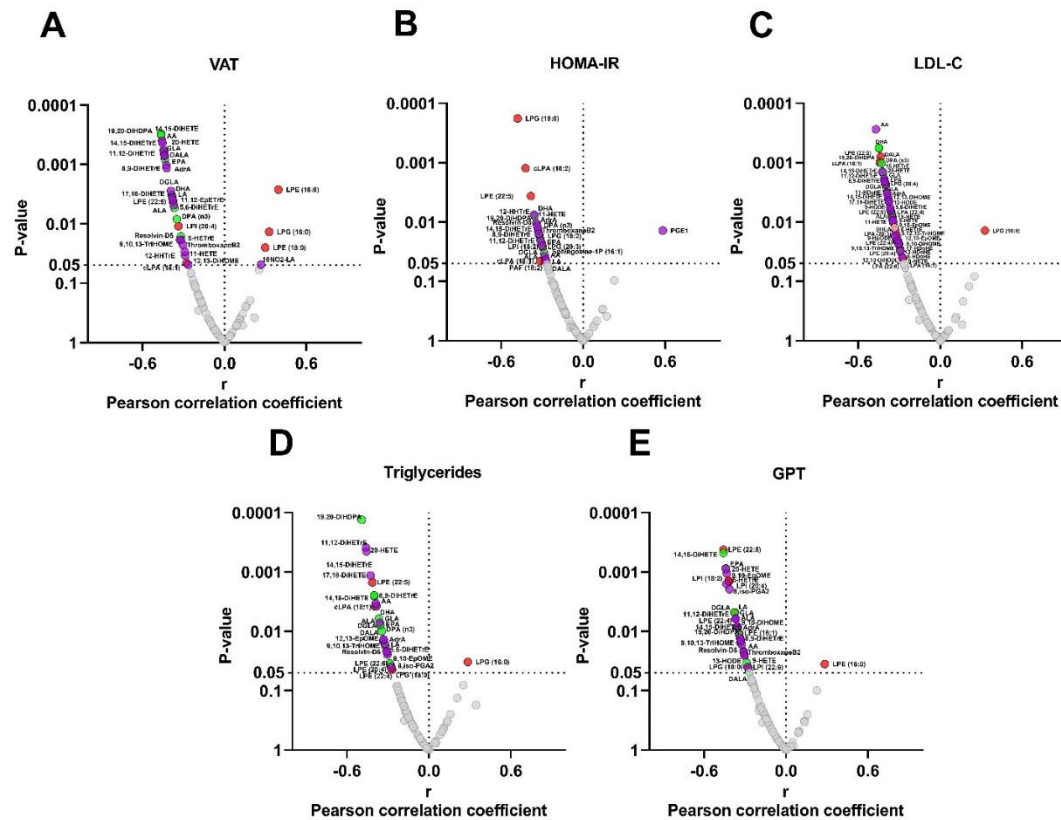


**Figure S12. Association between cold-induced changes in the plasma levels of signaling lipids and cardiometabolic risk parameters. Related to Figure 4.**

Volcano plots showing partial correlation analyses between the 120 min fold-change relative to baseline and VAT (A), HOMA-IR (B), LDL-C (C), triglycerides (D) and GPT (E). Partial correlation analyses were adjusted for the natural calendar day when the baseline 18F-FDG-PET/CT scan was performed. The X-axis represents Pearson partial correlation coefficients, whereas the Y-axis represents the FDR-adjusted P-values of the correlations. Grey dots represent non-significant correlations, whereas colored dots represent statistically significant correlations ( $P$ -value $<0.05$  after FDR correction). Abbreviations: GTP, glutamic pyruvic transaminase; HOMA-IR, homeostatic model assessment of insulin resistance index; LDL-C, low-density lipoprotein cholesterol; VAT, visceral adipose tissue.

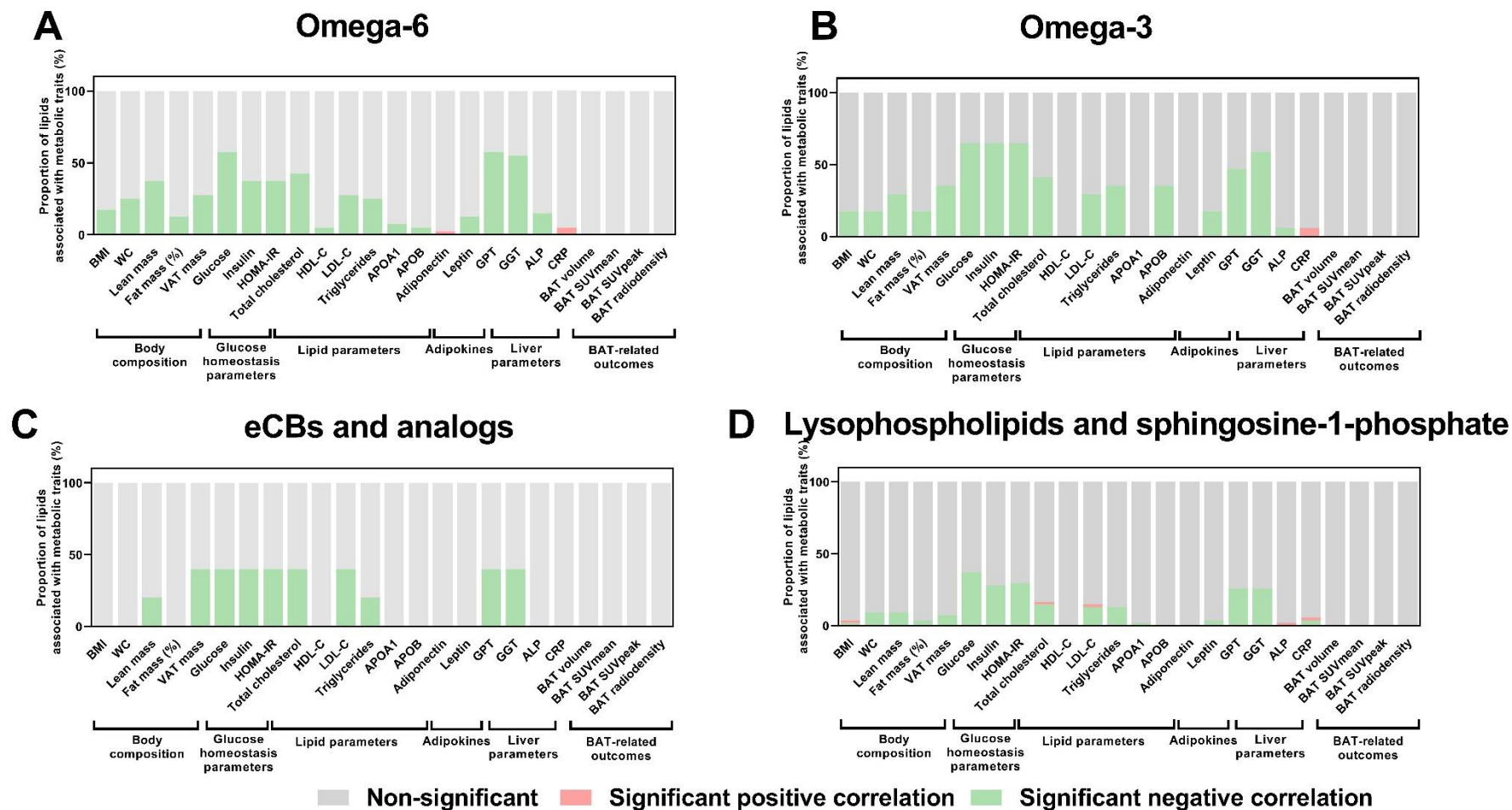


Figure S13. Relationship of cold-induced changes on the plasma levels of signaling lipids with cardiometabolic risk factors and brown adipose tissue in men (n=17). Related to Figure 4.



Bar graphs showing the proportion of cold-induced changes in omega-6 oxylipins (A), omega-3 oxylipins (B), endocannabinoids (eCBs, C), and lysophospholipids and sphingosine-1-phosphate species (D) associated with cardiometabolic risk factors. Associations were determined by Pearson bivariate correlation analyses or partial correlation analyses (for brown adipose tissue). Partial correlation analyses were adjusted for the natural calendar day when the baseline <sup>18</sup>F-FDG-PET/CT scan was performed. Cold-induced changes in plasma lipidome were determined by the 120 min fold-change relative to baseline. Significance was set at P-value<0.05 after FDR correction. Grey parts represent the proportion of lipids showing non-significant correlations, red parts represent the proportion of lipids showing significant positive correlations, whereas green parts represent the proportion of lipids showing significant negative correlations. *Abbreviations:* ALP, alkaline phosphatase; APOA1, apolipoprotein A1; APOB, apolipoprotein B; BAT, brown adipose tissue; BMI, body mass index; CRP, C-reactive protein; eCBs, endocannabinoids; GGT, gamma-glutamyl transferase; GPT, glutamic pyruvic transaminase; HDL-C, high-density lipoprotein cholesterol; HOMA-IR, homeostatic model assessment of insulin resistance index; LDL-C, low-density lipoprotein cholesterol; SUV, standardized uptake value; VAT, visceral adipose tissue; WC, waist circumference.

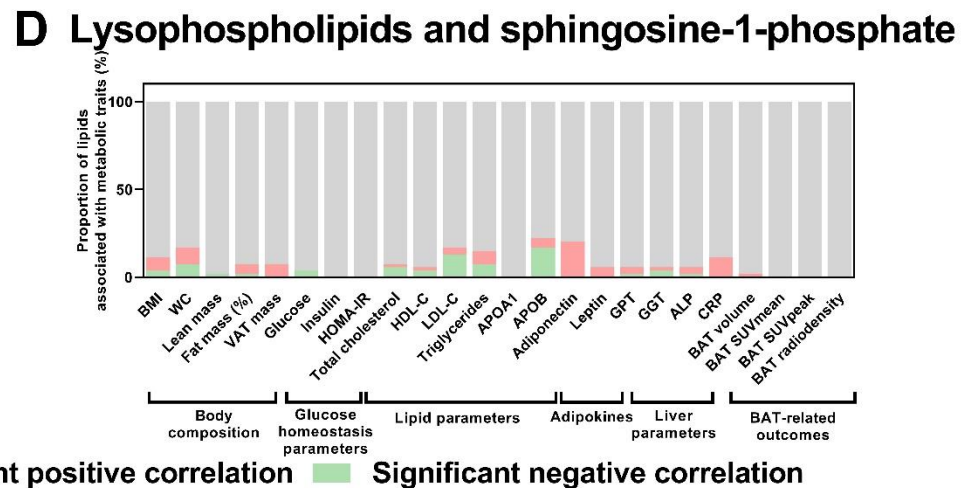
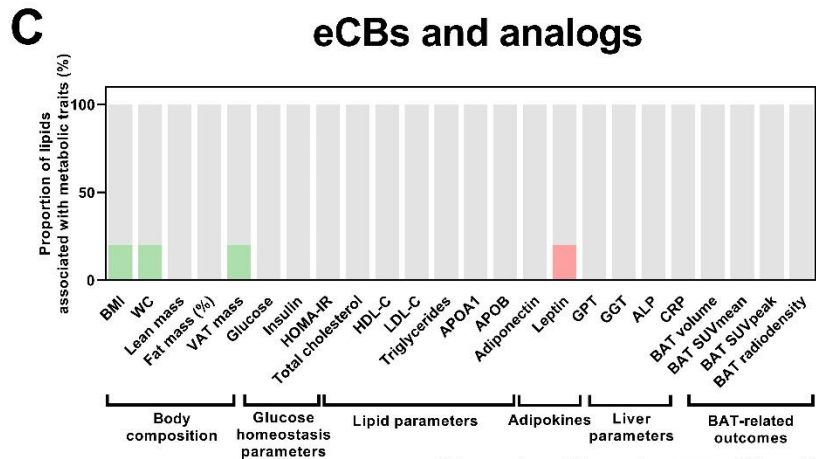
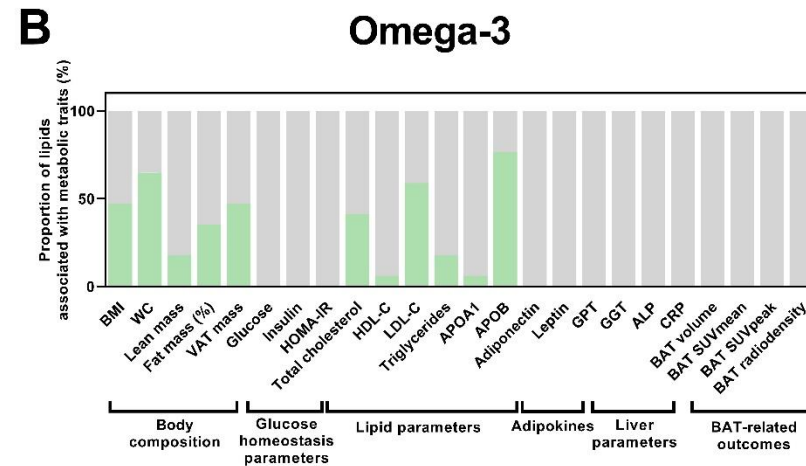
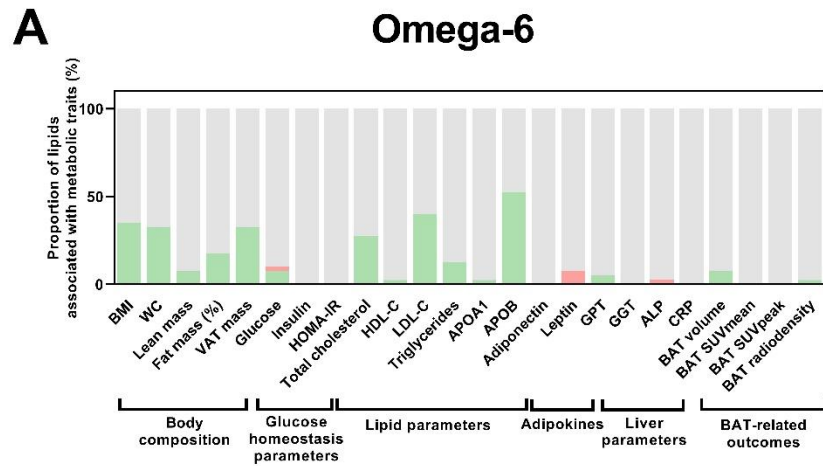


Figure S14. Relationship of cold-induced changes on the plasma levels of signaling lipids with cardiometabolic risk factors and brown adipose tissue in women (n=47). Related to Figure 4.

Bar graphs showing the proportion of cold-induced changes in omega-6 oxylipins (A), omega-3 oxylipins (B), endocannabinoids (eCBs, C), and lysophospholipids and sphingosine-1-phosphate species (D) associated with cardiometabolic risk factors. Associations were determined by Pearson bivariate correlation analyses or partial correlation analyses (for brown adipose tissue). Partial correlation analyses were adjusted for the natural calendar day when the baseline <sup>18</sup>F-FDG-PET/CT scan was performed. Cold-induced changes in plasma lipidome were determined by the 120 min fold-change relative to baseline. Significance was set at P-value<0.05 after FDR correction. Grey parts represent the proportion of lipids showing non-significant correlations, red parts represent the proportion of lipids showing significant positive correlations, whereas green parts represent the proportion of lipids showing significant negative correlations. *Abbreviations:* ALP, alkaline phosphatase; APOA1, apolipoprotein A1; APOB, apolipoprotein B; BAT, brown adipose tissue; BMI, body mass index; CRP, C-reactive protein; eCBs, endocannabinoids; GGT, gamma-glutamyl transferase; GPT, glutamic pyruvic transaminase; HDL-C, high-density lipoprotein cholesterol; HOMA-IR, homeostatic model assessment of insulin resistance index; LDL-C, low-density lipoprotein cholesterol; SUV, standardized uptake value; VAT, visceral adipose tissue; WC, waist circumference.

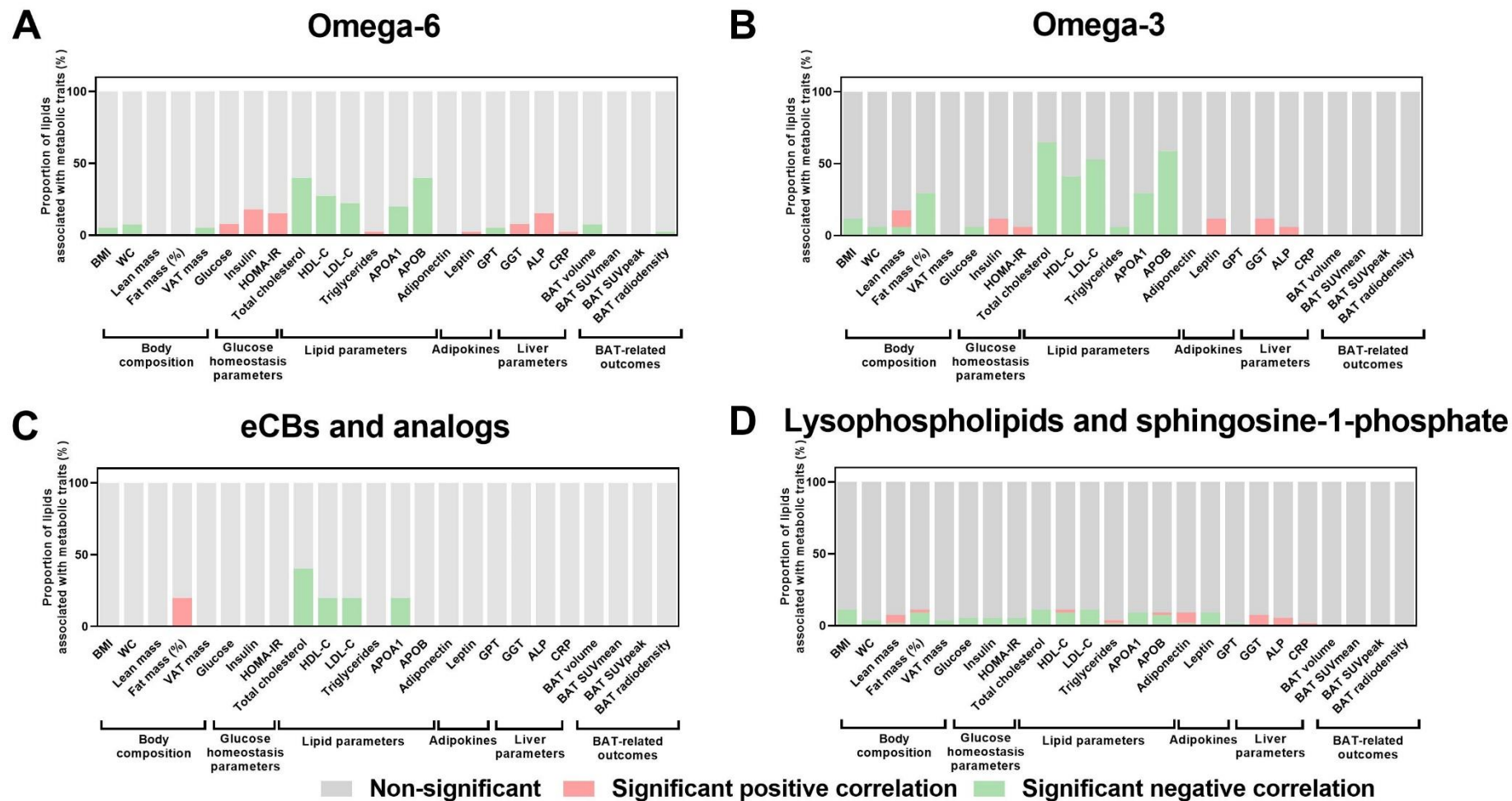


Figure S15. Relationship of cold-induced changes on the plasma levels of signaling lipids with cardiometabolic risk factors and brown adipose tissue in participants with normal-weight (n=43). Related to Figure 4.

Bar graphs showing the proportion of cold-induced changes in omega-6 oxylipins (A), omega-3 oxylipins (B), endocannabinoids (eCBs, C), and lysophospholipids and sphingosine-1-phosphate species (D) associated with cardiometabolic risk factors. Associations were determined by Pearson bivariate correlation analyses or partial correlation analyses (for brown adipose tissue). Partial correlation analyses were adjusted for the natural calendar day when the baseline <sup>18</sup>F-FDG-PET/CT scan was performed. Cold-induced changes in plasma lipidome were determined by the 120 min fold-change relative to baseline. Significance was set at P-value<0.05 after FDR correction. Grey parts represent the proportion of lipids showing non-significant correlations, red parts represent the proportion of lipids showing significant positive correlations, whereas green parts represent the proportion of lipids showing significant negative correlations. *Abbreviations:* ALP, alkaline phosphatase; APOA1, apolipoprotein A1; APOB, apolipoprotein B; BAT, brown adipose tissue; BMI, body mass index; CRP, C-reactive protein; eCBs, endocannabinoids; GGT, gamma-glutamyl transferase; GPT, glutamic pyruvic transaminase; HDL-C, high-density lipoprotein cholesterol; HOMA-IR, homeostatic model assessment of insulin resistance index; LDL-C, low-density lipoprotein cholesterol; SUV, standardized uptake value; VAT, visceral adipose tissue; WC, waist circumference.

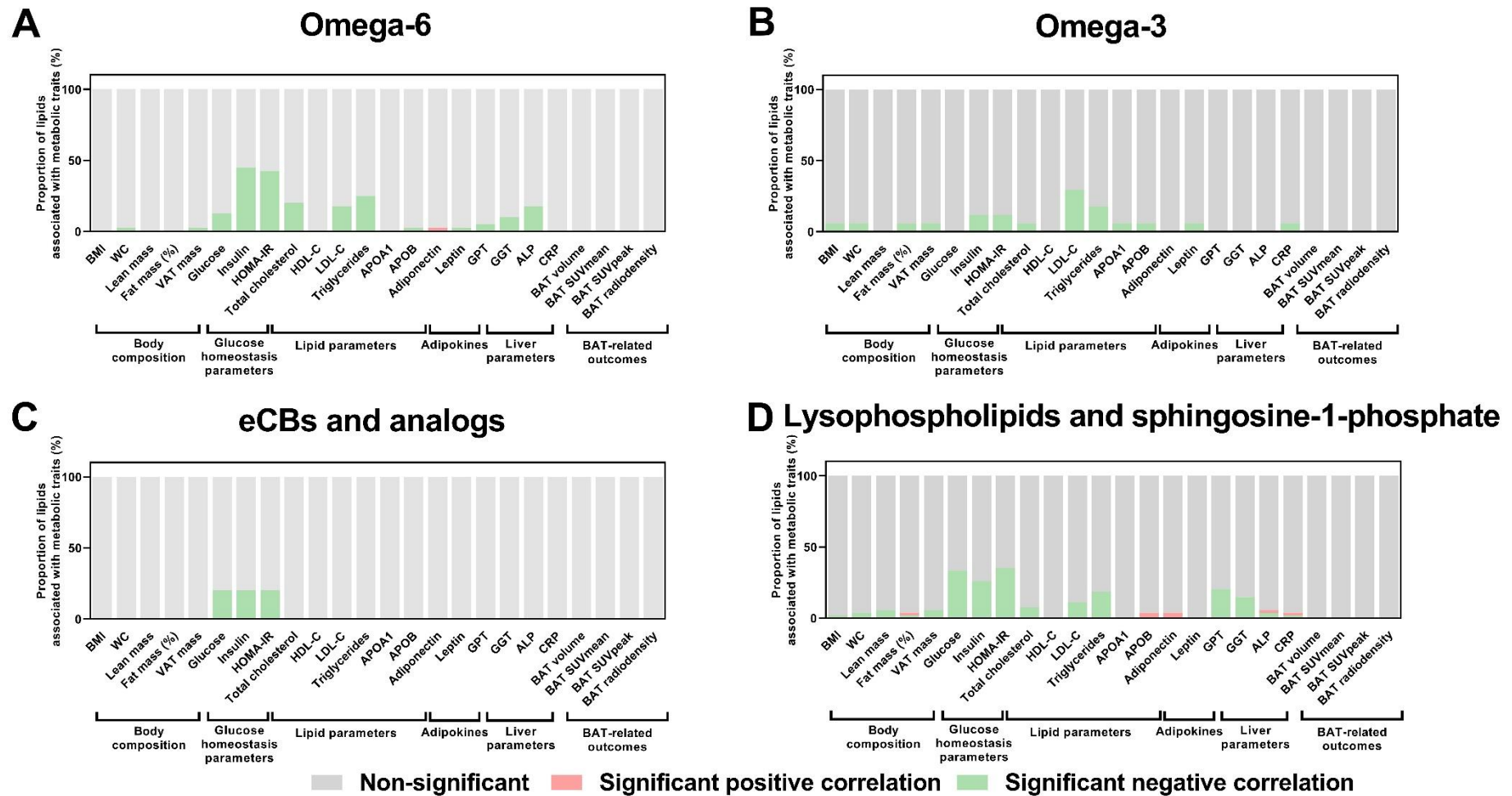
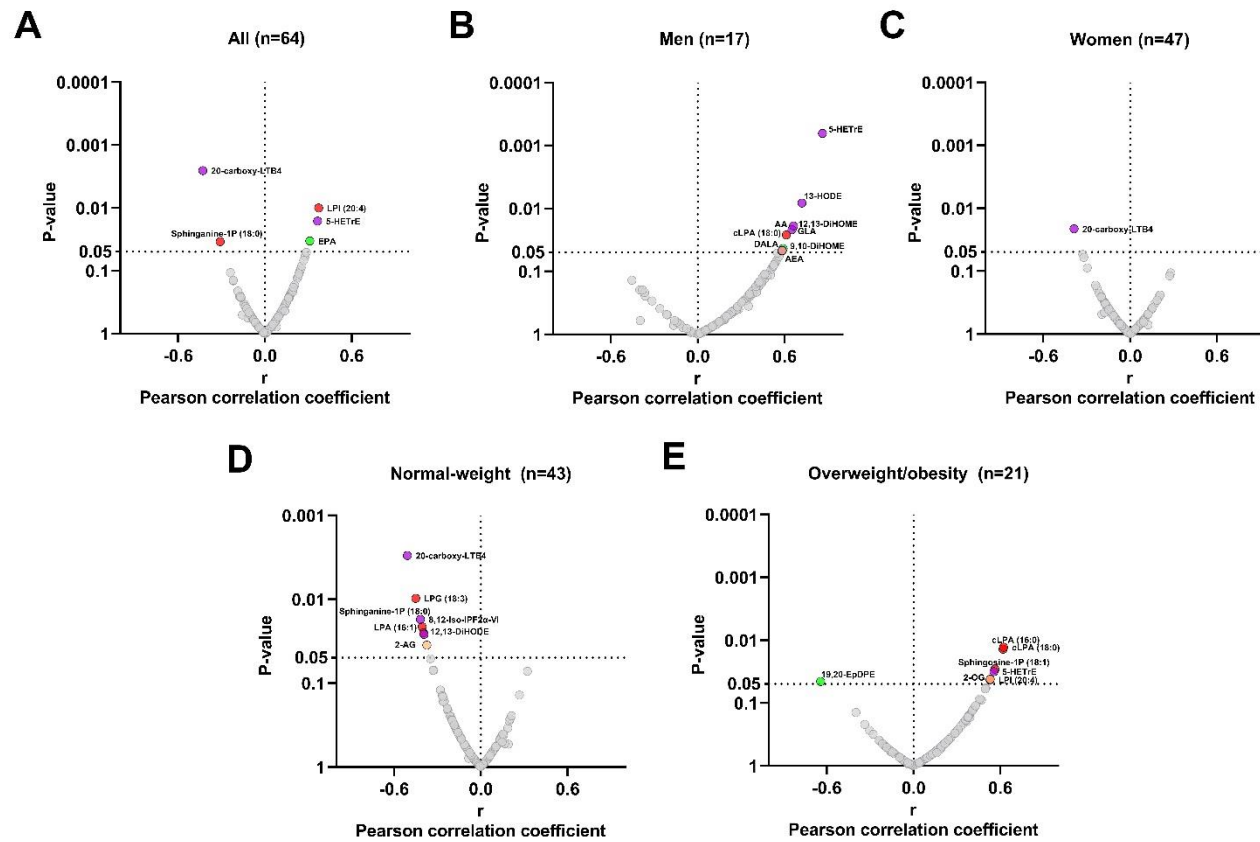


Figure S16. Relationship of cold-induced changes on the plasma levels of signaling lipids with cardiometabolic risk factors and brown adipose tissue in participants with overweight/obese (n=21). Related to Figure 4.

Bar graphs showing the proportion of cold-induced changes in omega-6 oxylipins (A), omega-3 oxylipins (B), endocannabinoids (eCBs, C), and lysophospholipids and sphingosine-1-phosphate species (D) associated with cardiometabolic risk factors. Associations were determined by Pearson bivariate correlation analyses or partial correlation analyses (for brown adipose tissue). Partial correlation analyses were adjusted for the natural calendar day when the baseline <sup>18</sup>F-FDG-PET/CT scan was performed. Cold-induced changes in plasma lipidome were determined by the 120 min fold-change relative to baseline. Significance was set at P-value<0.05 after FDR correction. Grey parts represent the proportion of lipids showing non-significant correlations, red parts represent the proportion of lipids showing significant positive correlations, whereas green parts represent the proportion of lipids showing significant negative correlations. *Abbreviations:* ALP, alkaline phosphatase; APOA1, apolipoprotein A1; APOB, apolipoprotein B; BAT, brown adipose tissue; BMI, body mass index; CRP, C-reactive protein; eCBs, endocannabinoids; GGT, gamma-glutamyl transferase; GPT, glutamic pyruvic transaminase; HDL-C, high-density lipoprotein cholesterol; HOMA-IR, homeostatic model assessment of insulin resistance index; LDL-C, low-density lipoprotein cholesterol; SUV, standardized uptake value; VAT, visceral adipose tissue; WC, waist circumference.



**Figure S17. Association between cold-induced changes on the plasma levels of signaling lipids and the water temperature of the cooling vest. Related to Figures 3 and 4.**

Volcano plots showing correlation analyses between 120 min fold-change rel. to baseline and water temperature of the cooling vest in all participants (A), men (B), women (C), normal-weight (D), and overweight/obese (E). The X-axis represents Pearson correlation coefficients, whereas the Y-axis represents the FDR-adjusted P-values of the correlations. Grey dots represent non-significant correlations, whereas colored dots represent statistically significant correlations (P-value < 0.05 after FDR correction).



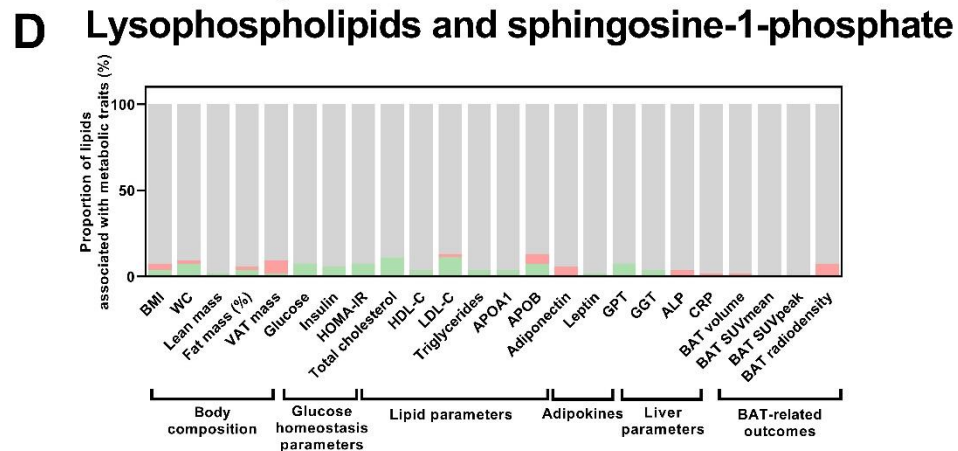
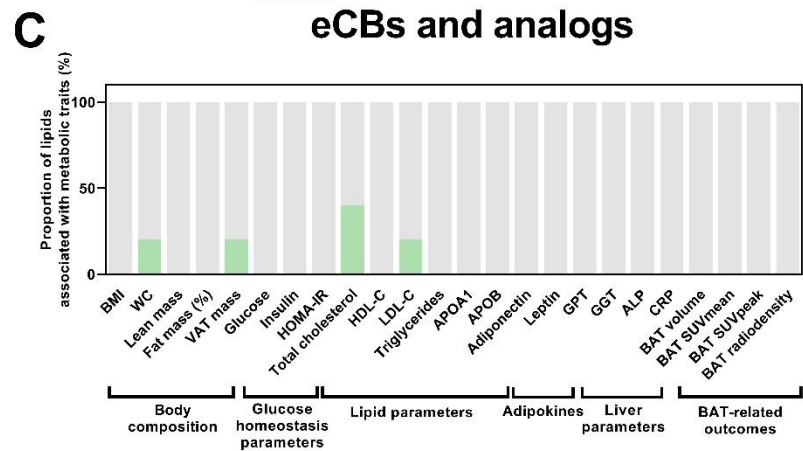
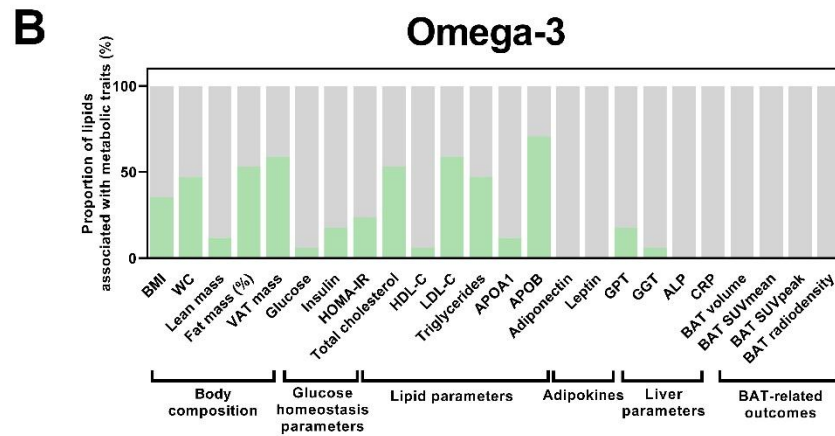
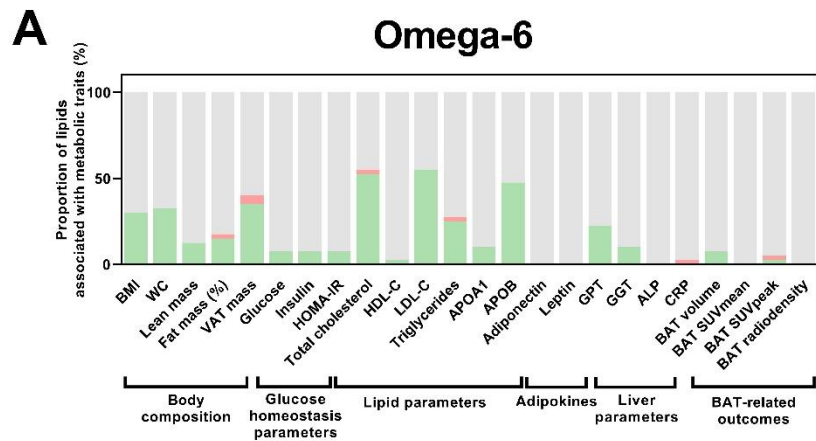


**Figure S18: Relationship of cold-induced changes on the plasma levels of signaling lipids with cardiometabolic risk factors and brown adipose tissue adjusting for the water temperature of the cooling vest. Related to Figure 4.**

Bar graphs showing the proportion of cold-induced changes in omega-6 oxylipins (A), omega-3 oxylipins (B), endocannabinoids (eCBs, C), and lysophospholipids and sphingosine-1-phosphate species (D) associated with cardiometabolic risk factors. Associations determined by Pearson partial correlation analyses adjusted for the water temperature of the cooling vest and for both the water temperature of the cooling vest and the natural calendar day when the baseline  $^{18}\text{F}$ -FDG-PET/CT scan was performed (for brown adipose tissue). Cold-induced changes in plasma lipidome were determined by the 120 min fold-change relative to baseline. Significance was set at  $P$ -value $<0.05$  after FDR correction. Grey parts represent the proportion of lipids showing non-significant correlations, red parts represent the proportion of lipids showing significant positive correlations, whereas green parts represent the proportion of lipids showing significant negative correlations. *Abbreviations:* ALP, alkaline phosphatase; APOA1, apolipoprotein A1; APOB, apolipoprotein B; BAT, brown adipose tissue; BMI, body mass index; CRP, C-reactive protein; eCBs, endocannabinoids; GGT, gamma-glutamyl transferase; GPT, glutamic pyruvic transaminase; HDL-C, high-density lipoprotein cholesterol; HOMA-IR, homeostatic model assessment of insulin resistance index; LDL-C, low-density lipoprotein cholesterol; SUV, standardized uptake value; VAT, visceral adipose tissue; WC, waist circumference.